Engineering 20 (2023) 162–179

Contents lists available at ScienceDirect

Engineering

journal homepage: www.elsevier.com/locate/eng

Research
Civil Engineering Material—Review

Hydration Characteristics and Microstructure of Alkali-Activated Slag Concrete: A Review

Qiang Fu [a,b], Mengxin Bu [a,*], Zhaorui Zhang [a], Wenrui Xu [a], Qiang Yuan [c], Ditao Niu [a,b]

[a] School of Civil Engineering, Xi'an University of Architecture and Technology, Xi'an 710055, China
[b] State Key Laboratory of Green Building in Western China, Xi'an University of Architecture and Technology, Xi'an 710055, China
[c] School of Civil Engineering, Central South University, Changsha 410075, China

ARTICLE INFO

Article history:
Received 14 January 2021
Revised 31 May 2021
Accepted 28 July 2021
Available online 10 December 2021

Keywords:
Alkali-activated slag concrete
Hydration characteristics
Pore structure
Interfacial transition zone
Microstructure

ABSTRACT

Alkali-activated slag concrete (AASC) is a new green building material. The amount of CO_2 produced by AASC is 1/5th of that produced by ordinary Portland cement concrete (OPCC). In addition, AASC promotes the reuse of slag and other wastes and saves resources. Furthermore, the scope of use of slag has been expanded. The progress of the research on the hydration characteristics, microstructure, interfacial transition zone, and pore structure of AASC based on the relevant literatures was analyzed and summarized in this study. The influences of the slag composition, the type and dosage of the alkali activator, and the curing conditions on the hydration characteristics and the microstructure of the AASC were discussed. Relatively few research results on the microstructure of AASC are available, and the relevant conclusions are not completely consistent. Moreover, there are many constraints on the development of AASC (e.g., complex composition of raw materials of slag, large shrinkage deformation, and low fluidity). Therefore, further research is required.

1. Introduction

At present, ordinary Portland cement concrete (OPCC) is the most widely used building material. As the raw material of OPCC, the demand for ordinary Portland cement is increasing annually because of the continuous expansion of infrastructure construction. However, the production of ordinary Portland cement requires enormous quantities of resources and releases a huge amount of CO_2. It has been established statistically that approximately one ton of CO_2 is released for each ton of cement produced. The global cement industry emits approximately 1.35 Gt of CO_2 annually, which accounts for 7% of the total anthropogenic emissions [1–6]. Therefore, it is an urgent problem for the construction industry to identify a green and environmentally friendly cement substitute to reduce the environmental pollution caused by cement production.

In recent years, the research on alkali-activated materials (AAMs) based on cementitious materials has been a popular topic in academic circles. AAMs can yield higher environmental benefits because their manufacture results in the production of fewer greenhouse gases (particularly CO_2). In addition, the raw materials or precursors of AAMs are generally industrial byproducts or industrial wastes, which are not only inexpensive but also beneficial to waste reuse. Relevant studies have revealed that certain industrial solid wastes become highly active with an alkali activator, which provides conditions for strength development [7–10]. Moreover, the mechanical properties, temperature resistance, and corrosion resistance of AAMs are superior to those of ordinary Portland cement-based materials [11–15]. Therefore, AAMs have attracted widespread attention since their origination and they are currently the substitute for cement-based materials with the most potential.

Slag is the main raw material of alkali-activated slag concrete (AASC). It is an active mineral material with potential hydraulicity. The annual global output of slag is nearly 320 Mt [16]. However, only part of this output is used in the production of cement and concrete and with good results. Therefore, slag is the preferred material for achieving green energy saving, low-carbon emissions, and environmental protection for the concrete industry. The calcium content of slag is higher than those of the precursors of other types of alkali-activated concrete (such as fly ash, metakaolin, and silica fumes), which thereby accelerates the formation of early

* Corresponding author.
E-mail address: bumengxinsdjn@163.com (M. Bu).

https://doi.org/10.1016/j.eng.2021.07.026

hydration products with the activation of the alkali activator. Moreover, higher strength can be achieved due to the polycondensation reaction of the silica and alumina precursor [17,18]. In addition, the content of MgO in slag is relatively high, which contributes to the formation of hydrotalcite ($Mg_6Al_2(OH)_{16}CO_3$) with activation by an alkali activator and which plays an important role in the development of the early strength of AASC. Therefore, the properties of AASC including the mechanical properties, temperature resistance, and chemical corrosion resistance are better than those of other alkali-activated concrete. Furthermore, AASC has the advantages of high setting speed and high early strength, which can advance the time of remolding, improve the production speed of prefabricated components, speed up the project progress, and reduce the project cost [19–22]. In addition, the hydration heat of AASC is low, which is why AASC can be used extensively in mass concrete engineering. Moreover, the particles of slag powder are finer than cement particles and they can better fill in the pores of hydration products, whereby AASC has a denser internal structure.

AASC is a ceramic-like material with an amorphous to semi-crystalline three-dimensional (3D) aluminosilicate structure. After the raw materials that are rich in silicon and aluminum are activated by a mixed alkaline solution, the dissolved AlO_4 and SiO_4 tetrahedra combine to form monomers by sharing an oxygen atom. The monomers then interact to form oligomers, which are subsequently polymerized to form a 3D network of aluminosilicate structures, as shown in Fig. 1 [23]. The microstructure of AASC has an important influence on its macroscopic properties such as the mechanical properties, dimensional stability, and durability. The formation mechanism of the macro properties of AASC can be comprehended by studying its microstructure. Therefore, the macroscopic properties of AASC can be adjusted by altering its microstructure appropriately. This study summarizes the research results on the hydration characteristics and microstructure of AASC that have been obtained in recent years to provide a theoretical basis for regulating the macroscopic properties of AASC.

2. Fundamental components and preparation technology of alkali-activated slag concrete

2.1. Fundamental composition

The raw materials of AASC include slag, fine aggregate, coarse aggregate, water, alkali activator, and admixture. The most common slag is ground granulated blast furnace slag (GGBFS). Nonferrous metal slag, steel slag, and iron slag can also be used as raw materials for AASC. GGBFS is waste slag produced during ironmaking, and it is ground after being quenched with water. It is the main solid waste in the ferrous metallurgical industry, and it has a special silicate structure [24,25]. The chemical composition of GGBFS varies with the ironmaking method and the type of iron ore. It can be represented by the $CaO–SiO_2–Al_2O_3–MgO$ quaternary phase diagram [11]. The fine and coarse aggregates of AASC are mostly sand and stone. However, in recent years, a few researchers have used steel slag sand and electric arc furnace (EAF) slag as fine and coarse aggregates, respectively, to prepare high-performance AASC [26]. Glukhovsky et al. [27] divided alkali activators into six categories according to their chemical composition: ① caustic alkali: MOH, ② non-silicate weak acid salt: M_2CO_3, M_2SO_3, and so forth, ③ silicate: $M_2O{\cdot}nSiO_2$, ④ aluminate: $M_2O{\cdot}nAl_2O_3$, ⑤ aluminosilicate: $M_2O{\cdot}Al_2O_3{\cdot}(2–6)SiO_2$, and ⑥ non-silicate strong acid salt: M_2SO_4. However, most researchers use NaOH, Na_2CO_3, Na_2SiO_3, and Na_2SO_4 as alkali activators because these are conveniently available. A few researchers mix NaOH and Na_2SiO_3 in a certain ratio to be used as an alkali activator to obtain better

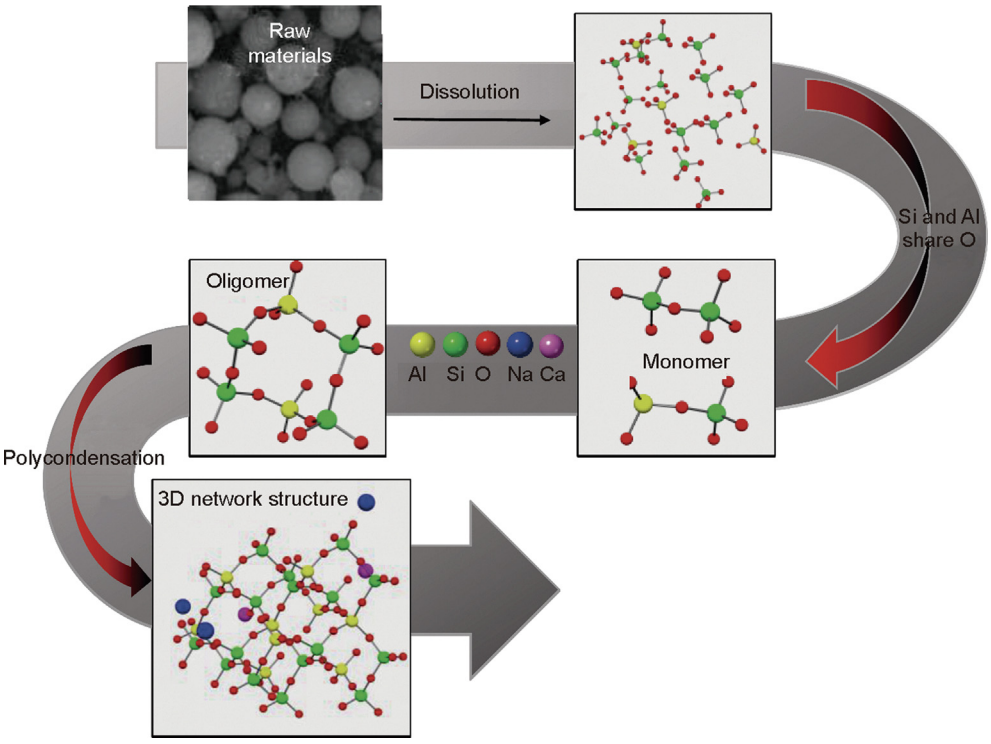

Fig. 1. Geopolymerization process for AASC [23].

activated effects. However, in recent years, with consideration of the fact that some alkali activators (such as NaOH and sodium silicate) may cause high carbon emissions in the production process, these can be replaced with some green alkali activators (such as Na_2CO_3, Na_2SO_4, Bayer solution, sodium aluminate, lime, and rice husk ash) [28–35].

2.2. Preparation technology

The preparation of AASC is similar to that of OPCC. The main differences are in terms of ① whether an alkali activator is added or not and ② the method and time of adding the alkali activator. In most studies, a liquid alkali activator was used as the catalyst and added in the mixing process. Jin et al. [36] studied the influence of an alkali activator mixing method on the hydration of slag. The study showed that the mixing sequences of the alkali activator and water were divided into pre-mixing and post-mixing (pre-mixing refers to the process in which the alkali activator and water are mixed outside the ampoule before being lowered into the calorimeter, and post-mixing is the process in which the alkali activator and water are lowered into the calorimeter separately and mixed in the ampoule immediately before the measurement). A negative heat flow was investigated when the post-mixed sequence was applied, whereas it was not observed for the pre-mixing sequence. This could be attributed to the recombination of silicate.

Solid alkali activators can be used in addition to liquid alkali activators. The research results of Shi et al. [11] showed that a solid alkali activator could be added using three methods: ① The solid alkali activators are dissolved in water, and then the ground slag is mixed with the alkali activator solution, ② the alkali activators are ground together with slag, and ③ the alkali activators and slag are ground separately and mixed together before being mixed with water. Method ① is widely used because the alkali activator and slag can be mixed together uniformly and certain active points on the surface of the slag can adsorb certain alkali activators to enhance the activity of the slag. However, certain alkali activators may be hydrolyzed during grinding and storage. In this case, it is more appropriate to use method ②.

The preparation of AASC depends more on the curing conditions. Similar to the curing conditions of OPCC, those of AASC generally include the curing time, curing temperature, humidity, and steam pressure. Similar to OPCC, the hydration degree, density, and strength of AASC increase with the increase in the curing time, and the early growth is faster [37]. The curing temperature has a substantial influence on the formation and morphology of the slag hydration products. An appropriate increase in the curing temperature can complete the activation of the hydraulic properties of the cementitious material within a short curing time. Without an alkali activator and only using thermal activation, slag powder can yield a corresponding strength within a certain period of time, and the morphology of the hydration products develops well [38]. Therefore, the curing temperature is highly important to the development of the hydration products and strength of AASC. With regard to the curing humidity, Collins and Sanjayan [39] immersed AASC in water, sealed it, and exposed it to air for curing. It was found that the sample cured in water had high early strength, and the strength continued to increase at 365 days. However, the strength was low and stopped growing at 90 days when cured under sealed conditions. The main reason for this was that the slag inside the specimen does not have the moisture required for hydration. Therefore, humidity is also an important factor that affects the hydration and strength development of AASC. The strength of AASC develops rapidly with autoclave curing, its hydration products have a relatively stable structure, and it has strong high-temperature resistance.

3. Hydration characteristics of AASC

3.1. Hydration process

The hydration process of slag can be divided into five stages: preinduction period, induction period, acceleration period, deceleration period, and stable period, as shown in Fig. 2. This process is identical to that of ordinary Portland cement. However, slag is regarded as a material with low heat of hydration, and the heat of hydration of slag is lower than that of ordinary Portland cement [27,40]. The hydration process of AASC can be summarized as follows: ① dissolution of vitreous body particles, ② nucleation and growth of the initial solid phase, ③ mechanical bonding and interaction of the new phase at the interface, and ④ diffusion and chemical equilibrium of the reaction products at the initial stage of curing [41–43]. A large number of studies [30,44–51] have demonstrated that the composition of slag, the type and dosage of the alkali activator, and the curing conditions have substantial influence on the hydration process of AASC.

3.1.1. Effect of slag composition on hydration process

The composition can directly affect the hydration process and hydration products of slag. Although the chemical composition of different slag is almost similar, the chemical components content of slag is very different. Shi et al. [11] discovered that the contents of SiO_2 and CaO in slags from different countries were similar, whereas those of Al_2O_3, MgO, and TiO_2 varied substantially. The composition of slag would affect its activity and thereby its hydration process. Relevant studies have shown that the mass ratio $m_{CaO+MgO}/m_{SiO_2+Al_2O_3}$ can be used as an effective indicator of the slag reaction performance. Glass slag with a m_{CaO}/m_{SiO_2} mass ratio of 0.5–2.0 and $m_{Al_2O_3}/m_{SiO_2}$ mass ratio of 0.1–0.6 is considered to be the most suitable precursor of AAMs [36,52].

Slag with a higher content of Al_2O_3 would reduce the dissolution rate of SiO_2 and other components, which would result in a lower heat of hydration in the early stage. However, the intensity and the time of the second hydration peak also have certain relationships with the alkali activator. Haha et al. [51] studied the effect of different Al_2O_3 contents (7.0%, 14.1%, and 16.7%) of slag on the hydration process of slag, as shown in Fig. 3. Irrespective of whether Na_2SiO_3 or NaOH was used as the alkali activator, the slag with a higher content of Al_2O_3 resulted in a lower cumulative heat evolved for the slag. In addition, the second hydration reaction peak was delayed when Na_2SiO_3 was used as the alkali activator, whereas the converse was true for NaOH. Tänzer et al. [24] used NaOH and K_2SiO_3 separately as alkali activators to study the effect of different Al_2O_3 contents of slag on the hydration process. It was discovered that the slag with a high content of Al_2O_3 resulted in a low cumulative heat evolved for slag. Gruskovnjak et al. [53] studied the hydration process of slag with Al_2O_3 contents of 7.7% and 11.5%. They reported that the slag with the Al_2O_3 content of 11.5% had a short dormancy period and a strong second hydration reaction peak. Sakulich et al. [54] found that a marginal dosage of Al_2O_3 in slag could accelerate the hydration process. However, slag with an Al_2O_3 content of 15% or higher delayed the hydration process and reduced the heat of hydration.

In addition to the content of Al_2O_3, the contents of MgO and TiO_2 in slag can affect the hydration process of slag. However, the relevant research results are relatively few, and consensus has not been attained. The slag with a higher MgO content has a higher alkalinity. The cumulative heat evolved and the degree of hydration increase when slag dissolves completely. However, a higher TiO_2 content would reduce the slag dissolution rate, which would have a negative impact on the hydration process. Haha et al. [55] studied the effect of various MgO contents in slag (8%, 11%,

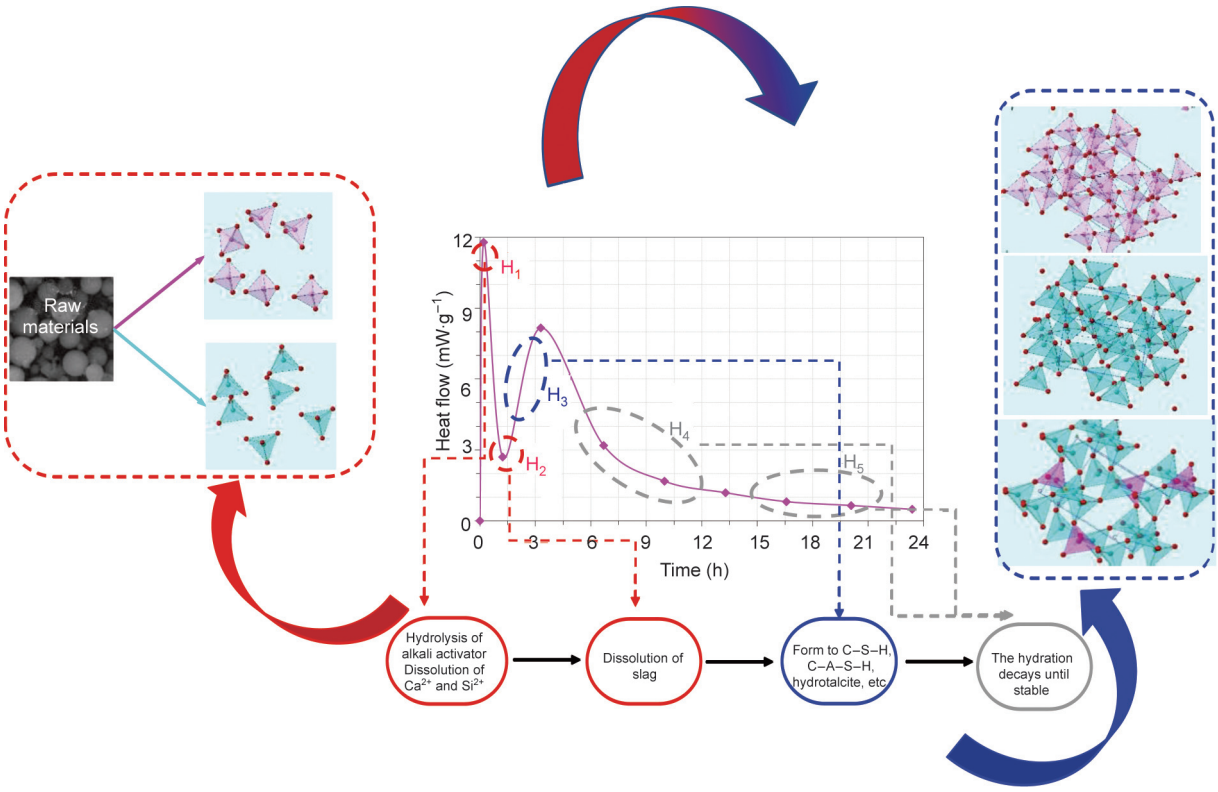

Fig. 2. Hydration process of slag. H_1 is preinduction period, H_2 is induction period, H_3 is acceleration period, H_4 is deceleration period, and H_5 is stable period.

and 13%) on the hydration process of slag. It was observed that the hydration degree of slag decreased with the increased content of MgO in the first 24 h when NaOH was used as the alkali activator, while the results were the opposite when Na_2SiO_3 was used as the alkali activator or for other hydration periods when NaOH was used as the alkali activator. Bernal et al. [56] indicated that reducing MgO content in slag accelerated the early hydration reaction process of slag, but the overall hydration extent of slag decreased. Ke et al. [57] studied the influence of the MgO content in slag on the hydration process of slag. They found that a high MgO content of slag could shorten the setting time and improve the hydration reaction rate. Tänzer et al. [24] studied the influence of various TiO_2 contents in GGBFS (0.5% and 1.9%) on the hydration process (Fig. 4). GGBFS with a higher TiO_2 content had a lower hydration heat, and its second hydration peak was delayed when Na_2SiO_3 was used as the alkali activator. Nevertheless, the cumulative heat that evolved was almost unaltered. When NaOH was used as the alkali activator, the GGBFS with the high TiO_2 content evolved a higher cumulative heat. This might be attributed to the fineness of the GGBFS. Katya et al. [58] found that TiO_2 content of 2% inhibited the hydration reaction rate of C_3S. Thereby, the hydration reaction rate of slag with a high TiO_2 content was slower, and the cumulative heat that evolved was lower.

The influence of the slag composition on the hydration process of slag can be summarized as follows. The slag dissolution exotherm will accelerate the dissolution of slag in the early stage of the hydration reaction when the Al_2O_3 content in slag is low. Alternatively, the production of ettringite (AFt) in super sulfate slag and Portland cement slag can increase the intensity of the second hydration reaction peak. However, an excessive Al_2O_3 content would reduce the dissolution of amorphous silica, quartz, and other components, which would delay the hydration process [59,60]. NaOH is a strong alkali. Therefore, Mg^{2+} that decomposes from slag can react with OH^- to produce $Mg(OH)_2$ precipitation in the early stage of the hydration reaction when NaOH is used as the alkali activator. The formation processes of hydrotalcite-like, brucite, and other hydration products are limited. As the hydration reaction progresses, a large amount of OH^- is consumed. $Mg(OH)_2$ is a weak electrolyte with an ionization balance. In consequence, the content of Mg^{2+} increases in the slag, which promotes the formation of hydration products such as hydrotalcite-like and brucite, and the degree of hydration improves. Hence, the hydration heat of slag with a high MgO content is lower in the first 24 h when NaOH is used as the alkali activator. However, the cumulative heat evolved is higher at or after 24 h, and Na_2SiO_3 as a type of salt may occur only when the alkali equivalent is adequately large. Ti exists in the form of six-coordination when the content of TiO_2 is less than 4%, but Ti exists in the form of four-coordination when the content of TiO_2 is more than 4%. Consequently, Ti has no significant effect on the activity of slag when the content of TiO_2 is less than 4%. The activity and dissolution rate of slag with a higher TiO_2 content are lower. Therefore, the cumulative heat evolved and the intensity of the second hydration reaction peak of slag with a high TiO_2 content are lower. In addition, Ti^{4+} and Ti^{3+} can replace Si^{4+} in the glass network, resulting in a denser glass structure, which can also affect the excitation effect of alkali activators (such as Na_2SiO_3 and NaOH).

3.1.2. Effect of alkali activator on hydration process

The type and dosage of the alkali activator can affect the hydration process of slag by affecting the pH value of the initial solution. Furthermore, the alkali activator can provide different ions for the hydration process and consequently affect the generation of specific hydration products and in turn, the hydration process. The hydrations of slag are highly different from those of ordinary Portland cement. Although the hydration exothermic curve of slag is similar to that of ordinary Portland cement for certain types of

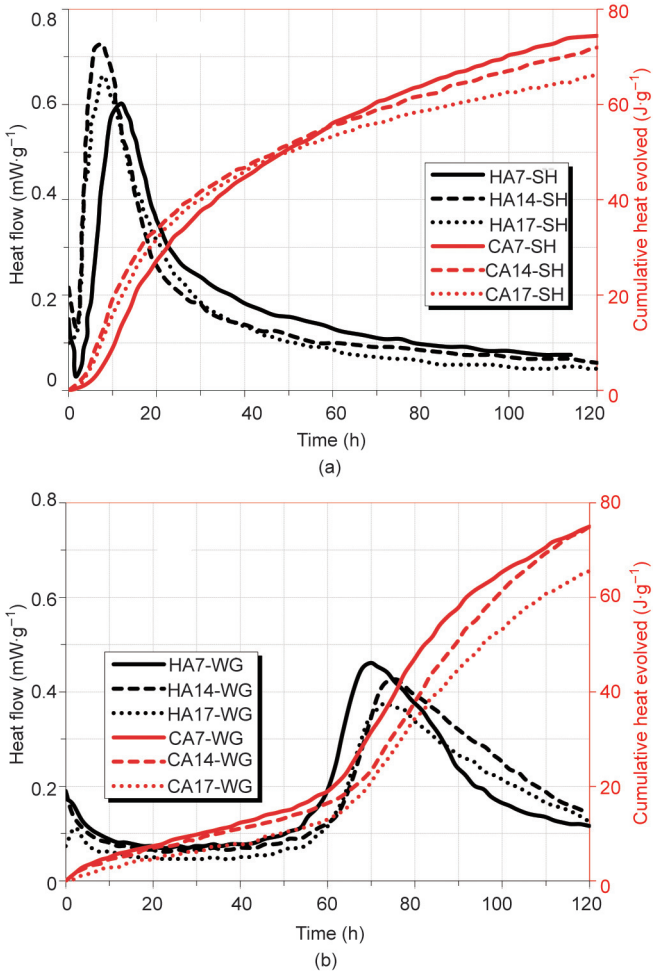

Fig. 3. Hydration evolution of the slag with different contents of Al_2O_3 using (a) sodium hydroxide (SH) and (b) water glass (WG) as alkali activator. H is heat flow, C is cumulative heat evolved, A is Al_2O_3, number is the contents of Al_2O_3, the same below [51].

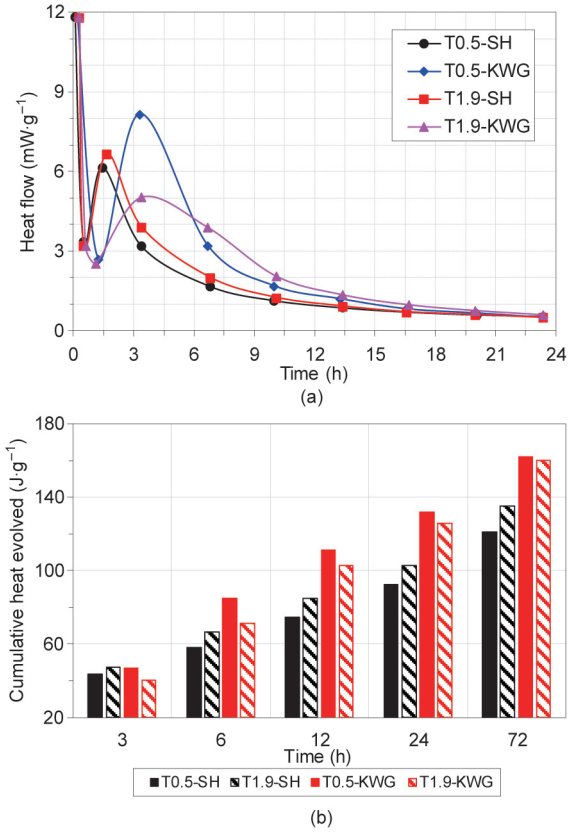

Fig. 4. (a) Heat flow and (b) cumulative heat evolved of GGBFS with different TiO_2 contents (T number, wt%) using SH and potassium silicate (KWG) as alkali activator [24].

alkali activators, the peak time and the peak strength are significantly different.

The pH value of the solution is higher when NaOH is used as the alkali activator with an identical alkali equivalent, accordingly which can dissolve slag faster, shorten the induction period, and accelerate the early hydration process of slag. Cao et al. [61] applied an ultrasonic monitoring system based on embedded piezoelectric transducers and used NaOH and Na_2SiO_3 as alkali activators to study the effect of alkali activators on the hydration process of slag (Fig. 5). The preliminary hydration reaction process of the slag using NaOH as the alkali activator was relatively straightforward. Its hydration exotherm curve was divided into three stages, and it had one hydration exothermic peak. This differed from the conclusion of many studies wherein there were two peaks in the hydration exothermic curve of slag when NaOH was used as the alkali activator [62–64]. Gijbels et al. [64] compared the effects of NaOH and Na_2SiO_3 on the hydration process of slag. They investigated the idea that the cumulative heat evolved of the slag was higher when NaOH was used as the alkali activator compared with Na_2SiO_3. The studies [7,41,46,55,65,66] also obtained a similar conclusion, which was related to the higher pH value of the initial solution when NaOH was used as the alkali stimulator for an identical alkali equivalent.

The dissolution rate of slag is slow because an Na_2SO_4 or Na_2CO_3 solution is nearly neutral, which delays the second hydration reaction peak of the slag. However, the pH value of the subsequent pore solution varies, which will cause the alteration of the slag hydration process in the subsequent stage. Tan et al. [67] performed a comparative study of the effects of Na_2SO_4 and Na_2CO_3 on the hydration process of slag. It was observed that for an identical alkali equivalent, the second hydration reaction peak of the slag was delayed significantly, the peak intensity was low, and the activation effect was poor when Na_2SO_4 was used as the alkali activator (Fig. 6 [67]). The studies [68–72] indicated that the hydration induction period of the slag was longer when Na_2SO_4 or Na_2CO_3 was used as the alkali activator compared with Na_2SiO_3 and NaOH.

The effects of alkali activators on the hydration process of slag can be summarized as follows. For an identical alkali equivalent, the pH value of an NaOH solution and the dissolution rate of slag are higher. Therefore, the slag has a shorter induction period and larger peak strength. The pH value, the intensity of the second hydration peak, and the cumulative heat evolved for an Na_2SiO_3 solution are lower than those of an NaOH solution. Na_2CO_3 and Na_2SO_4 are nearly neutral salts that are not conducive to slag dissolution. This restricts the initial solid phase nucleation and growth of the hydration products. Hence, the early peak strength for slag is lower than that of the former two, and the second hydration peak is delayed when Na_2CO_3 or Na_2SO_4 is used as the alkali activator. Nevertheless, the subsequent peak strength is similar to those of the former two. In addition, CO_3^{2-} that decomposes from Na_2CO_3 will combine with Ca^{2+} to form $CaCO_3$ precipitation before generating calcium alumina silicate hydrate (C–A–S–H) when Na_2CO_3 is used as the alkali activator, which will consequently delay the hydration process of the slag. With the consumption of CO_3^{2-} ions, the pH value of the pore solution increases, and the hydration process accelerates in the subsequent stage. It is

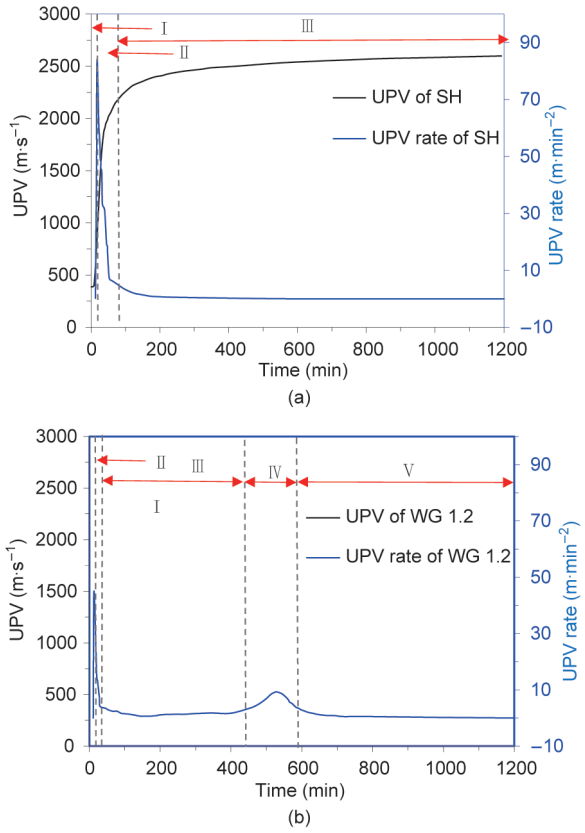

Fig. 5. The ultrasonic pulse velocity (UPV) evolution and UPV rate curves of slag using (a) SH and (b) Na_2SiO_3 (WG1.2, 1.2 is modulus (*Ms*)) as alkali activator [61]. I: dormancy stage; II: first acceleration stage; III: first deceleration stage; IV: second acceleration stage; V: second deceleration stage.

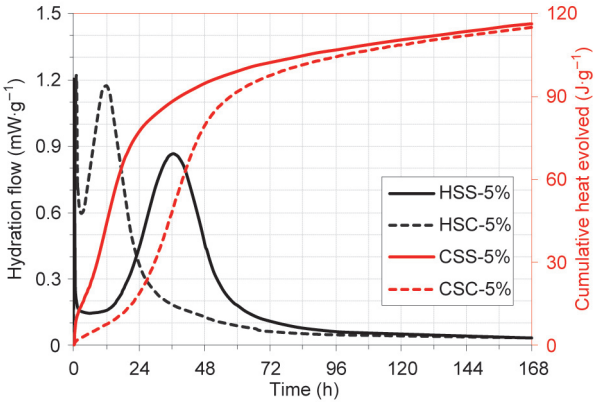

Fig. 6. Heat evolution of sodium sulfate (SS) and sodium carbonate (SC) with 5.0% Na_2O equivalent [67].

evident that the type and the dosage of alkali activator are comprehensively important factors that affect the hydration process of slag.

The parameter *n* (the mass ratio of Na_2O to slag) and *Ms* (the mass ratio of SiO_2 to Na_2O) can affect the dissolution of slag particles and the nucleation and growth of the initial phase when Na_2SiO_3 is used as the alkali activator. This, in turn, affects the hydration process of slag. Ravikumar and Neithalath [73] studied the influence of Na_2SiO_3 with different *n* and *Ms* on the slag hydration process, as shown in Fig. 7. The use of Na_2SiO_3 with a higher *n* or lower *Ms* would result in a higher peak value of the second hydration reaction of slag. Studies [73–75] have investigated the effect of Na_2SiO_3 with different *n* on the hydration process of slag. It was discovered that a single peak appeared (i.e., the initial peak coincided with the acceleration peak), and there was no apparent induction period when *n* was significantly high. Cao et al. [61] studied the effect of silicate with different *Ms* on the hydration process of slag. It was observed that the silicate with a higher *Ms* shortened the hydration induction period of slag when the alkali equivalent was identical and thereby advanced the hydration acceleration period, which could be attributed to the fact that silicate with a higher *Ms* can provide more SiO_4^{4-} ions to accelerate the production of hydration products. However, the opposite conclusion was obtained in other studies [74,75]. The studies [47,75–77] demonstrated that two accelerated exothermic peaks appeared when the alkali equivalent was constant and the *Ms* was high. The first accelerated exothermic peak appeared because the high alkalinity of the alkali activator solution promoted the formation of early products. The second accelerated exothermic peak appeared because the formation of the early hydration products resulted in a higher consumption of alkali, and in turn, the increase in the silica concentration. A higher silica concentration and lower pH value promoted the decomposition of calcium.

The pH value of the alkali activator can control the dissolution of the vitreous body slag and the subsequent condensation reaction, which has a substantial influence on the efficiency of the alkali activator [78,79]. Among the compounds containing sodium, the pH value (and thereby, the activation efficiency) of an NaOH solution is the highest when the alkali equivalent is constant. With the increase in the alkali equivalent, the peak value of the second hydration reaction and the cumulative heat evolved increase, and the hydration degree of the slag improves significantly. Therefore, the pH value should be at least 11.5 when NaOH is used as the alkali activator [79]. Mobasher et al. [67] studied the effect of Na_2SO_4 with different alkali equivalents on the hydration process of slag. It was determined that with the increase of the alkali equivalent, the hydration induction period shortened, the second hydration peak appeared earlier, and the peak strength increased. Tan et al. [67] studied the effect of Na_2SO_4 and Na_2CO_3 with different alkali equivalents on the hydration process of slag. It was observed that with the increase in the alkali equivalent, the peak intensity of the second hydration reaction peak of the slag and the cumulative heat that evolved increased, and the appearance time was advanced (Fig. 8 [67]).

In addition, the states of the alkali activator will also affect the hydration process of AASC. Overall, liquid alkali activators are the

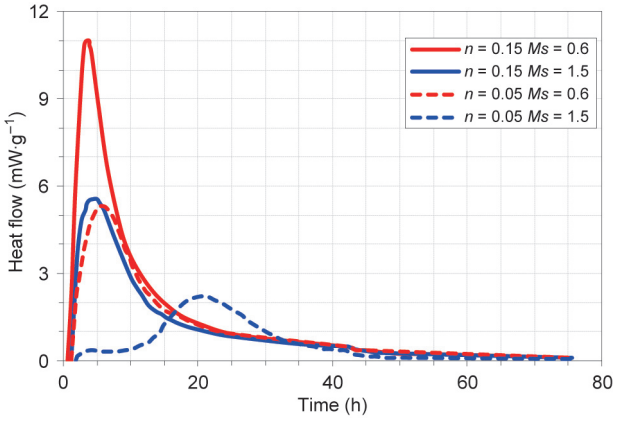

Fig. 7. Heat flow of slag using WG activator of different *n* and *Ms* as alkali activator [73].

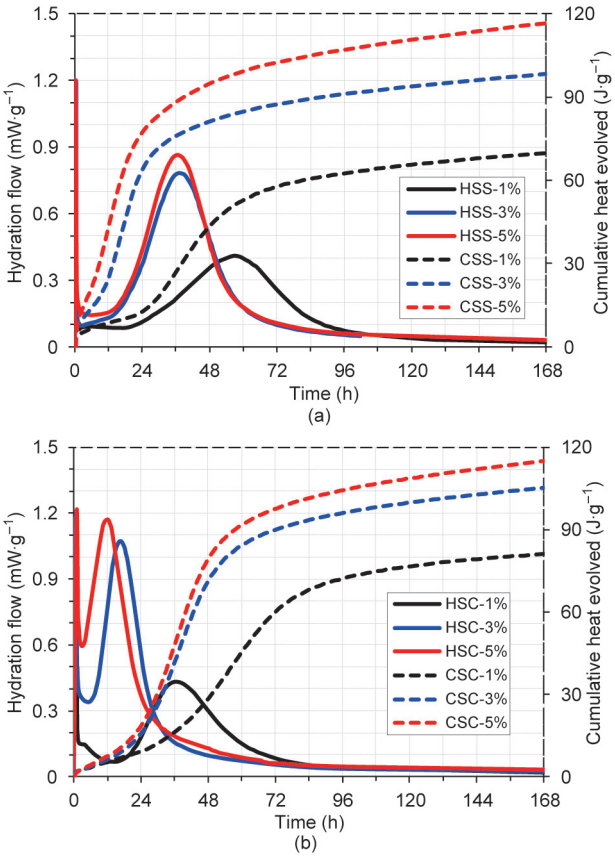

Fig. 8. Heat evolution of slag using (a) SS and (b) SC as alkali activator with different Na_2O-E [67].

activators that are used the most because a large amount of heat is generated when the solution is prepared. However, some researchers will choose solid alkali activators. For solid sodium hydroxide, the process of dissolution will release a large amount of heat. For water glass, the dissolution of anhydrous glass with *Ms* less than 2 or water glass is an exothermic process, and anhydrous glass with *Ms* more than 2 is an endothermic process. The larger the *Ms* is, the less alkali content in the glass there is, and the glass is more difficult to dissolve in water. The dissolution of anhydrous sodium carbonate and sodium carbonate monohydrate is exothermic, while the dissolution of sodium carbonate heptahydrate and sodium carbonate decahydrate is endothermic. The dissolution of anhydrous sodium sulfate is an exothermic process, and the dissolution of sodium sulfate decahydrate is an endothermic process [11]. The heat of dissolution will accelerate the dissolution of the slag and the hydration reaction, as well as increase the heat release at the initial stage of hydration when a solid activator is used.

The influence of the dosage of alkali activator on the hydration process of slag can be summarized as follows: After the slag dissolves, an aluminosilicate shell is rapidly formed on the surface of slag. The shell remains impermeable and the hydration reaction cannot be conducted until the shell is broken or dissolved. However, the shell can be better dissolved in a highly alkaline environment. Therefore, the highly alkaline alkali activator aids the production of hydration products. The second hydration reaction peak appears earlier and the peak intensity increases [44,45,79–83]. The peak intensity of the second hydration reaction peak is proportional to *n*/*Ms* when Na_2SiO_3 is used as the alkali activator. A higher *Ms* can provide more SiO_4^{4-} ions for the hydration reaction when the alkali equivalent is constant, which increases the amount of hydration products, resulting in higher cumulative heat being evolved and the formation of more hydration products.

3.1.3. Effect of curing technology on hydration process

Variations in the curing time, curing temperature, and curing humidity would result in alterations of the slag hydration process. An increase of the curing time improves the degree of hydration reaction, and an increase of the curing temperature can promote the hydration reaction of slag. However, the research on the influence of the curing humidity on the hydration process of slag is limited, and further research is required.

In general, the rate of the chemical reaction is doubled with every 10 °C increase in temperature. Similarly, an increase of the curing temperature can significantly accelerate the hydration process and increase the hydration exothermic rate of slag. Gijbels et al. [64] studied the effect of the curing temperature on the hydration process of slag. They observed that an increase of the curing temperature accelerated the hydration reaction process, advanced the second hydration reaction peak, and caused the peak to become higher and wider. This was consistent with the research results of Fernández-Jiménez and Puertas [84]. Gebregziabiher et al. [75] used NaOH and Na_2SiO_3 as alkali activators to study the effect of the curing temperature on the hydration process of slag. It was found that with a high curing temperature condition, the second hydration reaction peak of slag was advanced, and the peak intensity was improved, as shown in Fig. 9.

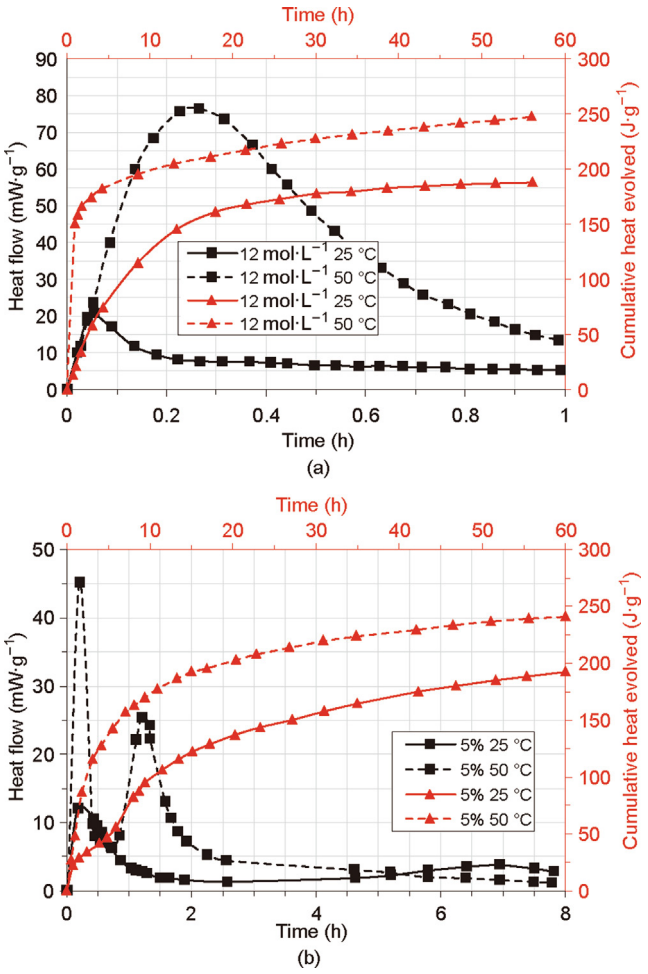

Fig. 9. Heat evolution of slag using (a) 12 mol·L^{-1} of SH and (b) 5% Na_2O of WG as alkali activator with different temperature [75].

3.2. Hydration products

Studies [46,61,68,78,85–90] have investigated and reported the hydration products of slag. C–(A)–S–H was generally considered to be the main hydration product of slag and it had a lower Ca/Si ratio, longer chain length, and higher degree of polymerization compared with the main hydration product of ordinary Portland cement (calcium silicate hydrate (C–S–H)). Thereby, it had higher strength. The higher alkalinity in the pore solution of AASC is conducive to penetrating the aluminosilicate shell on the slag surface, forming the secondary hydration products of C–S–H and C–A–S–H with higher alkali content, and increasing the internal C–S–H layer. However, the secondary hydration products of slag will vary with the composition, the type of alkali activator, and the curing conditions of slag.

3.2.1. Effect of slag composition on hydration products

The composition of slag, which is related to the iron and steel smelting process and ore sources, can affect the composition of hydration products and atomic ratio, replace the atoms in the C–S–H bridging position, alter the chain length of the hydration products, and affect the spatial structure of hydration products. Haha et al. [51] studied the effect of the Al_2O_3 content in slag on the hydration products of slag. It was discovered that the slag with a higher Al_2O_3 content increased the substitution of Al in C–S–H and formed C–A–S–H. However, the increase of the Al_2O_3 content in slag slowed down the early hydration rate, and the formation of hydration products was limited, which was consistent with the research results of Tänzer et al. [24]. According to the studies [49,55,56,78,86,88,91,92], hydrotalcite-like Mg–Al layered double hydroxides can also be observed in slag when the content of MgO is sufficient. The spatial structure is shown in Fig. 10. Gismondine ($CaAl_2Si_2O_8{\cdot}4H_2O$), phillipsite ($(K_2,Na_2,Ca)[AlSi_3O_8]_2{\cdot}6H_2O$), and so on will also be observed in AASC when the content of Al_2O_3 in the slag is high and that of MgO is low [43,93–95]. Yang et al. [96] studied the hydration products of slag doped with nano-TiO_2. They observed that no new hydration products were generated. However, the hydration product C–(A)–S–H of slag became denser.

The effect of the slag composition on hydration products can be summarized as follows. The hydration products of the slag mainly include brucite, hydrotalcite, and C–S–H when the content of Al_2O_3 in the slag is low and that of MgO is high. With the increase of the Al_2O_3 content in slag, the m_{Mg}/m_{Al} mass ratio of hydrotalcite decreases, and the number of C–A–S–H increases, which can be attributed to the fact that the increase of Al_2O_3 content in the slag results in the increase in the Al substitution for hydrotalcite and C–S–H. In addition, the increase of Al_2O_3 content in slag will reduce the concentration of oxides (i.e., CaO, SiO_2, MgO) as well as the amount of C–S–H and hydrotalcite, as shown in Fig. 11(a) [51]. C–(A)–S–H and hydrotalcite-like phase can be observed when the content of MgO in the slag is low. Brucite is also observed when the MgO content is high. Initially, more available Al is used to form a hydrotalcite-like material with the increase of MgO content in slag, whereby the amount of hydrotalcite-like material increases. Afterward, the remaining Al is incorporated into the C–S–H. Therefore, the substitution of Al in the C–S–H decreases, and the excess Mg^{2+} combines with OH^- to form brucite precipitation (Fig. 11(b)) [55].

3.2.2. Effect of alkali activator on hydration products

Many models of the main hydration product C–A–S–H of AASC are available, such as the tobermorite-like phase and the humite-like phase with different interlayer spacing. It has been indicated that the humite-like structure is similar to the main hydration product of slag when silicate is used as the alkali activator. A simple model of the tobermorite-like phase was developed by combining the research by Provis and Bernal [70] with the existing research on the C–A–S–H model, as shown in Fig. 12. The type of alkali activator would affect the structure and composition of the main hydration product C–A–S–H of slag as well as the formation of the secondary hydration products of slag.

Al appears mainly in the bridging position of C–S–H when NaOH is used as the alkali activator, which results in the restriction of the substitution degree of Al and the formation of Al-rich secondary

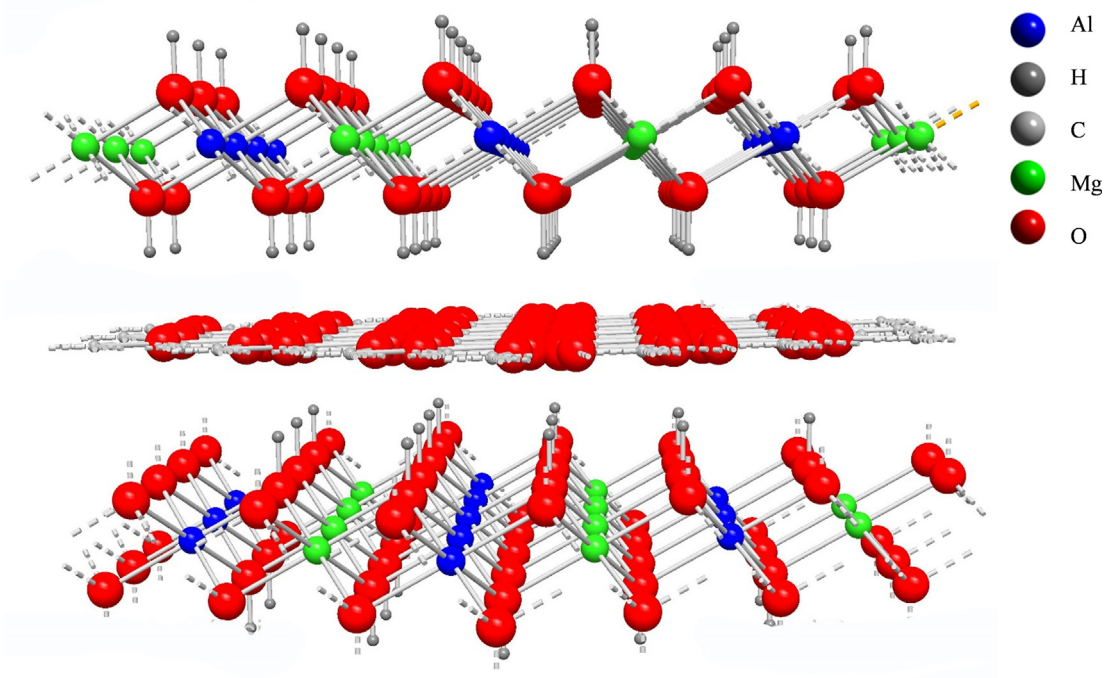

Fig. 10. Spatial structure of Hydrotalcite.

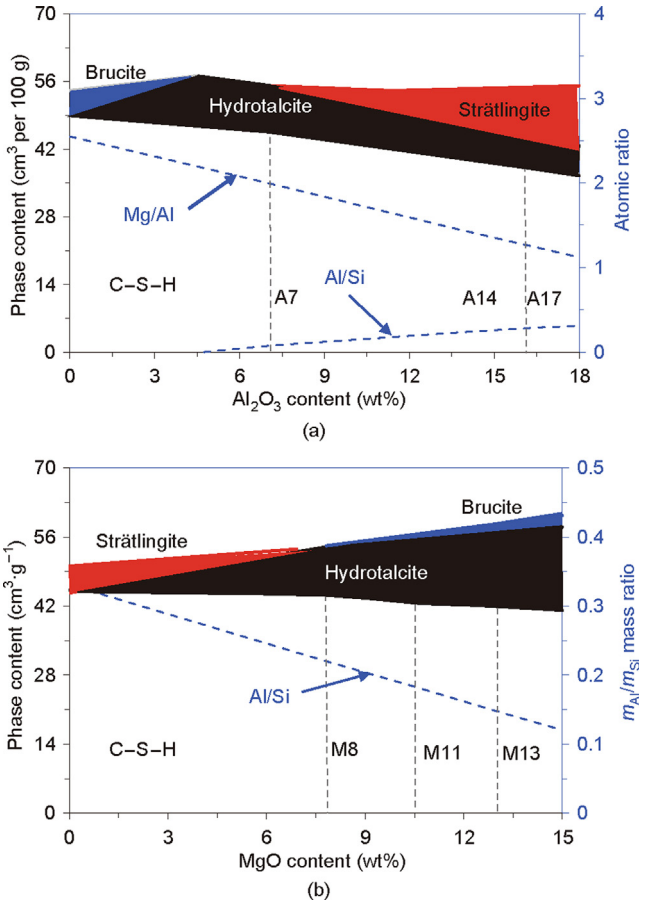

Fig. 11. Hydration products of slag with different (a) MgO contents [51] and (b) Al_2O_3 contents [55]. A7, A14, A17: Al2O3 content in slag; M8, M11, M13: MgO content in slag.

phases. The main hydration product of slag is C–A–S–H when NaOH is used as the alkali activator, which is similar to a tobermorite-like phase structure. Furthermore, Al exists mainly in the tetrahedral bridging position and has closely bound aluminum-rich second phases, such as hydrotalcite-like and AFt. Calcite ($CaCO_3$) is also observed, whereas the $Ca(OH)_2$ phase is not observed [61,79,88,91,97–102]. Schilling et al. [19] studied the hydration products of slag when NaOH was used as the alkali activator. C_4AH_{13} and hydrated calcium aluminosilicate (C_2ASH_8) were observed, and the intensity of the diffraction peak increased with the increase of the NaOH concentration and the hydration age.

Na_2SiO_3 can provide more SiO_4^{4-} for the polymerization process and produce C–A–S–H gel with a relatively high crosslinking degree. However, the crystallinity is relatively low, and the external hydration products increase because of the high SiO_2 concentration in the initial fluid region. Many studies [49,86,92,103,104] have demonstrated that when Na_2SiO_3 is used as the alkali activator, the main hydration product of slag is C–A–S–H with low crystallinity. Furthermore, nuclear magnetic resonance (NMR) has revealed that Na_2SiO_3 can induce the formation of C–A–S–H with relatively high Q_2 and Q_3 contents, a high degree of crosslinking, and good compactness. In addition, hydrotalcite-like, AFt, and other crystalline hydration products are produced in addition to C–(A)–S–H when Na_2SiO_3 is used as the alkali activator [105,106].

C–A–S–H, which is the main hydration product of slag, generally has a higher m_{Ca}/m_{Si+Al} mass ratio and a more ordered nanostructure when NaOH is used as the alkali activator compared with Na_2SiO_3 [105,106]. When NaOH is used as the alkali activator, some of the bonded Ca^{2+} in C–A–S–H may be replaced by Na^+, resulting in the formation of C–(N)–A–S–H [46].

The dissolved ions in slag can react with the ions provided by the alkali activator to promote the formation of specific reaction products. Na_2CO_3 and Na_2SO_4 solutions can provide different types of ions for the hydration of slag and thereby form different hydration products. Tan et al. [67] performed a comparative study of the influence of Na_2SO_4 and Na_2CO_3 as alkali activators for slag hydration products. They observed the appearance of AFt when Na_2SO_4 was used as the alkali activator, as shown in Fig. 13 [67]. This was consistent with the previous reports on slag hydration products [53,69,70,107–109]. Furthermore, the peak intensity of AFt at 28 days was lower than that at seven days, which was related to the carbonization of AFt. Calcite, calcium hemicarboaluminate (monosulfate (AFm)-like phase), manasseite (hydrotalcite-like phase), and gaylussite could be observed in the hydration products when Na_2CO_3 was used as the alkali activator. In addition, the peak value of the hydration products except for gaylussite increased at 28 d, which was consistent with the conclusion of the literature [68]. In addition, hydrotalcite and akermanite have been observed in the hydration products of slag when Na_2SO_4 is used as the alkali activator [68,69,109].

The effect of alkali activator on hydration products can be summarized as follows: C–(A)–S–H is the main hydration product of slag when different alkaline solutions are used as alkali activators. N–A–S–H and C–(N)–A–S–H also exist. The secondary hydration products are different for alkali activators. The use of NaOH as the alkali activator is favorable to the production of AFm, and the crosslinking degree of C–A–S–H is lower. Na_2SiO_3 can provide more SiO_4^{4-} when Na_2SiO_3 is used as the alkali activator, which causes the bridging unit of Si in C–A–S–H and the degree of polymerization of C–A–S–H to increase. It can decompose SO_4^{2-} ions when Na_2SO_4 is used as the alkali activator, and this can promote the production of AFt. More CO_3^{2-} can be produced by electrolysis when Na_2CO_3 is used as the alkali activator, and which can

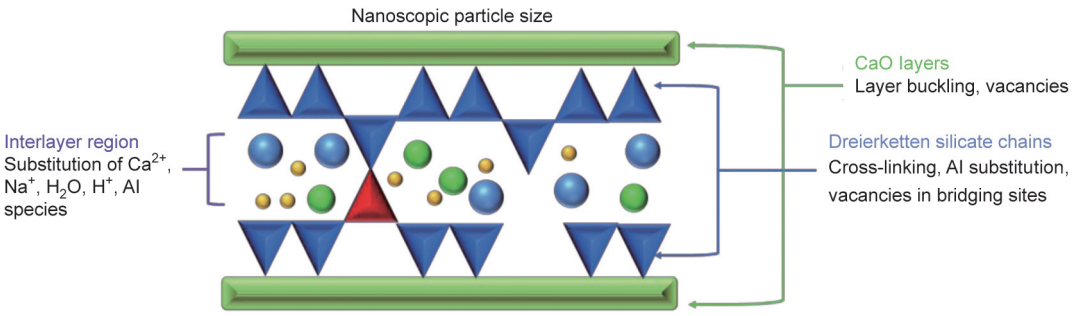

Fig. 12. Tobermorite-like C–A–S–H gel structure. The triangles denote tetrahedral Si sites (the red triangle denotes Al substitution into one bridging site), the green rectangles denote CaO layers, and the circles denote various interlayer species [70].

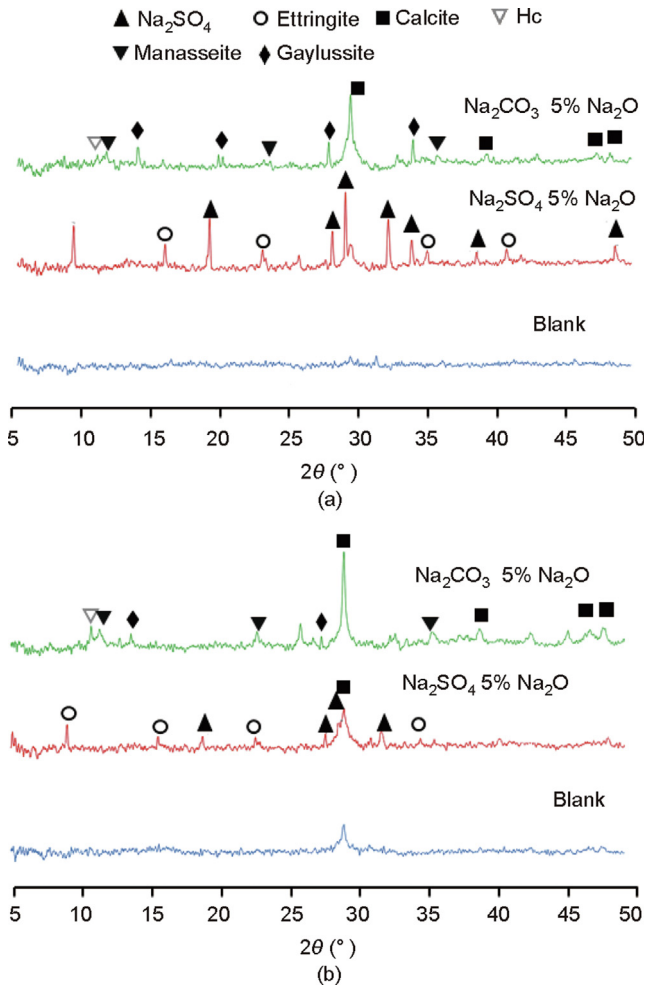

Fig. 13. X-rays diffraction pattern of GGBFS at (a) 7 d and (b) 28 d. 2θ: scatter angle. Reproduced from Ref. [67] with permission.

promote the formation of a $CaCO_3$ precipitation. The research results on the hydration products of slag with different alkali activators are relatively inconsistent, and the formation mechanism of the hydration products needs to be explored further.

3.2.3. Effect of curing conditions on hydration products

Although the main hydration products of slag under different curing conditions are similar, a variation in the curing conditions would alter the crystal structure of the hydration products and affect their crystallinity. The hydration products of slag with autoclave curing are significantly different from those obtained by curing under normal pressure. Well-crystallized crystals such as xonotlite, tobermorite, and natrolite (such as NaS_2H_3) are observed in the hydration products of slag under autoclave curing conditions [110]. Sugama and Brothers [111] studied the effect of the autoclave curing temperature on the hydration products of slag. It was observed that the main hydration product of slag with curing at 200 °C was C–S–H, whereas tobermorite and xonotlite with good crystallization were observed for 300 °C. Jiang [112] studied the effect of the curing temperature on slag hydration products. Only C–S–H and hydrotalcite were detected when the curing temperature was 25 °C. A series of well crystallized hydration products such as mica, nepheline, melilite, and sodium calcium silicate were formed when the curing temperature increased to 700 °C.

The effect of the curing conditions on the hydration products can be summarized as follows. An appropriate increase of the curing temperature can promote the hydration reaction and produce more hydration products with good crystallization. If the curing temperature is excessive, the free water will evaporate, and certain hydration products will be destroyed. Therefore, most of the hydration products will have a porous structure, which will cause them to be rough.

The hydration products of slag are determined mainly by the composition of slag, the type of alkali activator, the curing conditions, and so forth. Fig. 14 is a schematic diagram of the hydration products of AASC under different conditions [43,49,55,78,93,94,97,102–106,113].

4. Microstructure of AASC

4.1. Pore structure

AASC has a higher availability of silicon and lower m_{Ca}/m_{Si} mass ratio than OPCC. There are few large crystal grains with high solubility similar to $Ca(OH)_2$. Furthermore, the particle size of the hydration products is smaller, so the pores can be better filled, and the pore structure is optimized. Therefore, the pore structure of AASC is better than that of OPCC.

4.1.1. Effect of slag composition on pore structure

As has been established, large capillary pores and air pores are of substantial significance to the analysis of the compressive strength, flexural strength, and other mechanical properties of concrete. Gel pores and minute capillaries have a substantial influence on the shrinkage performance of concrete, particularly for AASC with poor drying shrinkage. Therefore, an analysis of the pore structure of AASC is of substantial significance to a further study of the mechanical properties, shrinkage properties, durability, and other properties of AASC. However, slag with different compositions would produce different hydration products, which would affect the pore structure of AASC. Therefore, it is necessary to analyze the influence of the slag composition on the pore structure.

As has been established, hydration products are of substantial significance to the filling of pores. This is particularly true for hydration products with a larger specific surface area, which have a significant impact on the refinement of the pore structure. Because the composition of slag can affect the formation of hydration products, a study of the composition of slag is highly important for analyzing pore structures. Wang et al. [114] studied the influence of slag with different MgO contents and different ages on the pore structure of AASC. They observed that slag with a low MgO content (LMg) would cause the porosity of AASC within the 1–50 nm pore size region to be lower. However, the average pore diameter was higher, which indicated that the content of the gel in the slag was low when the MgO content of the slag was low, as shown in Fig. 15 [114]. Yang et al. [96] studied the effect of the TiO_2 content in slag on the pore structure of AASC. They observed that slag with a high TiO_2 content resulted in a lower total porosity of AASC, so the AASC had a better pore size distribution. Ju et al. [115] studied the influence of slag with different CaO contents on the pore structure of AASC. They observed that the porosity of the AASC decreased with the increase of the CaO content in slag, which could be attributed to the fact that CaO could promote the hydration of the slag. Hence, more hydration products were generated, the number of micropores was reduced, and the pore structure became more compact. Wang et al. [116] studied the effect of the addition of nano-SiO_2 on the pore structure of AASC, as shown in Fig. 16. With the increase of the nano-SiO_2 content, the hydration reaction speed, quantity of hydration products of the AASC, and compactness increased, whereas the porosity decreased. Refs. [117,118] indicated that the number of pores

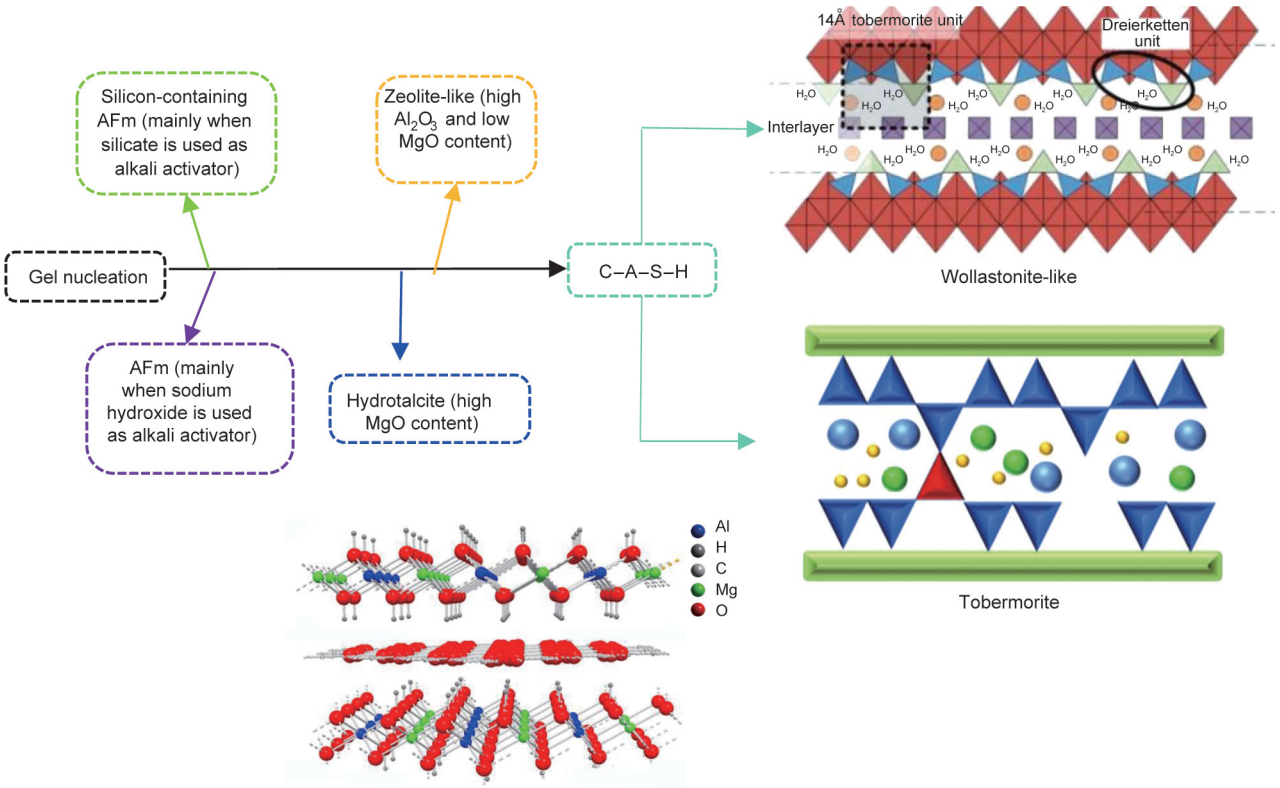

Fig. 14. Schematic diagram of hydration products of AASC under different conditions [43,49,55,78,93,94,97,102–106,113]. Reproduced from Ref. [113] with permission.

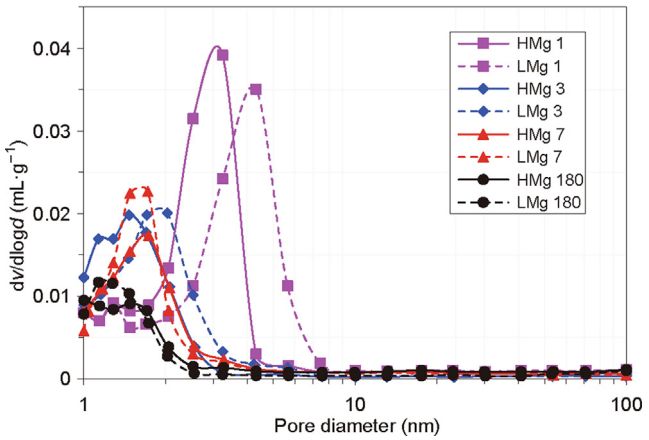

Fig. 15. Pore size distribution of AASC with different MgO content at different sample age (1, 3, 7, and 180 days) obtained using mercury intrusion porosimetry (MIP) [114]. HMg: high MgO content; LMg: low MgO content; *v* is cumulative pore volume; *d* is pore diameter; d*v*/dlog*d* can be regarded as the surface area of the pore.

larger than 30 μm in alkali-activated slag fly ash concrete was reduced substantially when the rate of quantity of slag and fly ash used to prepare the concrete was 4:1. This is because fly ash particles are smaller than slag particles, so they can better fill pores and optimize the pore structure. Hu et al. [119] studied the pore size distribution of alkali-activated slag/fly ash concrete with different slag/fly ash ratios. It was found that the porosity decreased with the increase of the slag/fly ash, and the proportion of 10–10^4 nm pores increased significantly since the addition of fly ash increased the content of high-porosity gel N–A–S–H gel in the gel and reduced the content of dense C–A–S–H gel, as shown in Fig. 17 [119].

The effect of the slag composition on the pore structure of AASC can be summarized as follows. The increase of non-expansive hydration products and the formation of phases with a larger specific surface area have a positive effect on improving the pore structure of AASC. Slag with a higher MgO content can promote AASC to produce more hydrotalcite-like phases with a larger specific surface area, it can better fill the pores and refine the pore structure. The dissolved TiO_2 exists as Ti^{4+} and Ti^{3+}, and it can be used as a network former to replace Si^{4+} and Ca^{2+} in the glass network. Ti^{3+} can strengthen the network, densify the glass structure, reduce the porosity of AASC, and improve the pore structure [24]. The increase of other substances in the slag, such as CaO, SiO_2, and so on can promote the production of C–(N)–A–S–H gel, thereby refining the pore structure. If nano-scale slag is used, as the fineness of the slag increases, the activity index of the slag increases, the hydration reaction is accelerated, the degree of hydration increases, and the hydration products are more uniform, which can significantly improve the pore structure of AASC.

4.1.2. Effect of alkali activator on pore structure

The content of macropores and mesopores decrease significantly with the formation of gelation and its filling effect as well as the induced nucleation effect of nanomaterials, which improves the pore size distribution and completely optimizes the microstructure. Nevertheless, this is closely related to the types and dosage of the alkali activators. The pore structures produced by different types of alkali activators display substantial differences.

The initial stage of the hydration reaction is affected by the dissolution of the vitreous body. An alkali activator with a high pH value can promote the dissolution of slag and accelerate the formation of hydration products, fill pores, and refine the pore structure. In the subsequent stage, the densification of the pore structure is

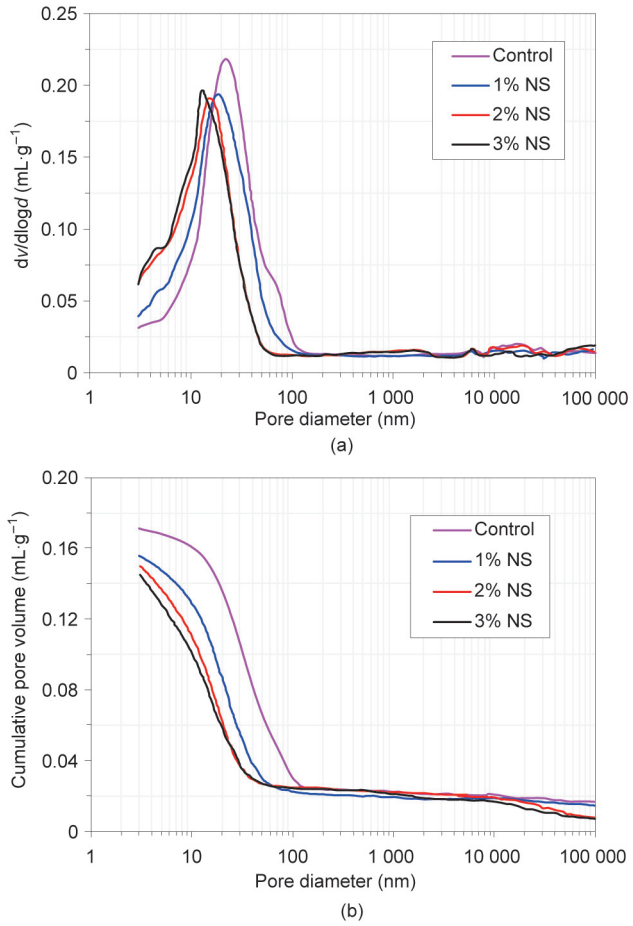

Fig. 16. (a) Pore size distribution and (b) cumulative pore volume of different nano silica (NS) contents (wt%) of AASC [116].

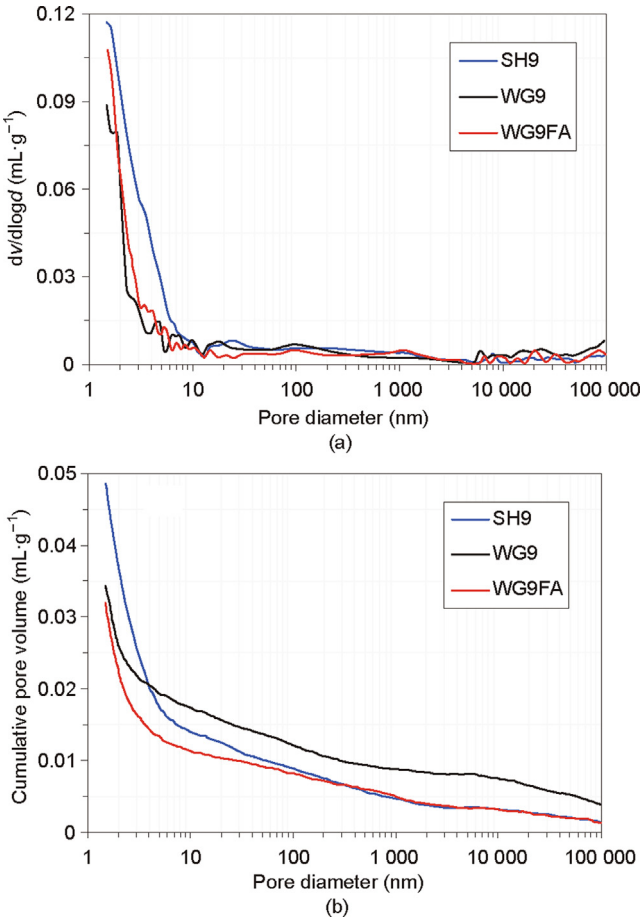

Fig. 18. (a) Pore size distribution and (b) cumulative pore volume of AASC with SH, NaSiO3 (WG), and WG/FA determined by MIP [117]. The number 9 is the Na_2O content (wt%). FA is referred to Fig. 17 [119].

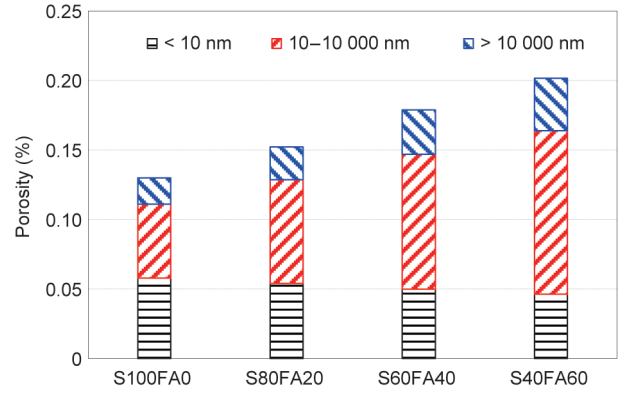

Fig. 17. Effect of fly ash content on the porosity and pore size distributions of alkali-activated slag/fly ash concrete. S: slag; FA: fly ash; the number is proportion of slag or fly ash, the same below [119].

mainly achieved by precipitation. The dissolution of the vitreous body in the early stage of the hydration reaction or the subsequent precipitation tremendously depend on the alkali activator. Zhang et al. [117] compared the effects of NaOH and Na_2SiO_3 on the pore structure of AASC, as shown in Fig. 18. The porosity of AASC was lower when Na_2SiO_3 was used as the alkali activator compared with NaOH. However, the number of pores larger than 10 μm was approximately 20 times that for the former, which might have been related to the microcracks caused by shrinkage. Gijbels et al. [64] studied the effect of NaOH content on the pore structure of AASC. They investigated the idea that with the increase of NaOH content, the porosity of AASC decreased and the pore structure became more refined. Hu et al. [120] studied the effect of alkali equivalents (4%, 6%, and 8%) on the pore structure of AASC when Na_2SiO_3 was used as the alkali activator. The results showed that with the increase in the alkali equivalent, the porosity of the AASC decreased, the proportion of micropores was higher than that of macropores, and the pore size distribution was better. With the increase of the curing time, the porosity decreased, and the porosity of the AASC was significantly lower than that of OPCC, as shown in Fig. 19 [120]. Ye et al. [121] compared the effects of NaOH and Na_2CO_3 on the pore structure of AASC. The study found that the porosity of AASC was lower when Na_2CO_3 was used as the alkali activator compared with NaOH. Jiao et al. [122] studied the effect of the Na_2CO_3/NaOH ratio on the pore structure of AASC. It was observed that with the increase in this ratio, the porosity and the mesopores of the AASC decreased, which could be attributed to the refining effect of Na_2CO_3 on the pore structure of AASC.

The effect of the alkali activator on the pore structure of AASC can be summarized as follows. The hydration reaction of slag is excessively fast when NaOH is used as the alkali activator, which causes a rapid formation of hydration products with relatively rough surfaces and non-uniform spatial dispersion; thereby, a poor pore structure will be formed. Na_2SiO_3 can provide more SiO_4^{4-} ions when it is used as an alkali activator, which is favorable to

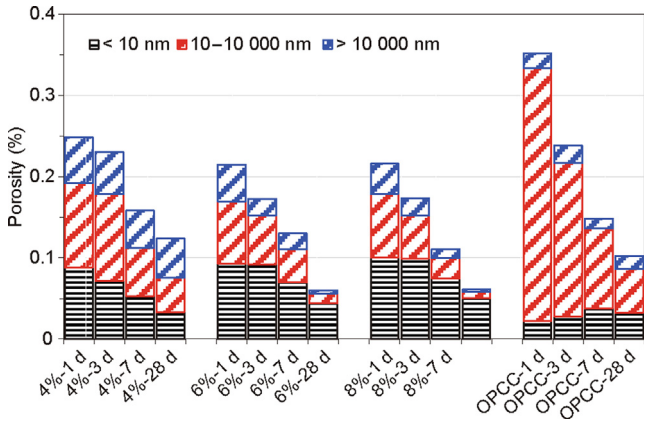

Fig. 19. Pore volume percentage at different alkali dosages and sample ages of AASC and OPCC [120].

the generation of hydration products. The Ca/Si ratio of C–(A)–S–H decreases when Na_2SiO_3 is used as the alkali activator. This, in turn, results in the improvement of the alkali binding capability of C–A–S–H, accelerates the hydration reaction, and generates more hydration products, a good pore size distribution, and a more compact matrix structure [83]. Therefore, the pore structure of AASC is better when Na_2SiO_3 is used as the alkali activator. The precipitate of $CaCO_3$ produced by the reaction between CO_3^{2-} ions in the alkali activator and Ca^{2+} dissolved in the slag can fill the pores better when Na_2CO_3 is used as the alkali activator. Moreover, with the consumption of CO_3^{2-}, the pH value in the pore solution increases, which is conducive to the formation of more hydration products and therefore optimizes the pore structure. The literature [46,80,83] reveals that the formation of hydration products depends on the availability of ions in the pore solution and its capability to penetrate the aluminosilicate shell. However, an alkali activator with a higher alkali equivalent can better penetrate the aluminosilicate shell attached to the slag surface and thereby further accelerate the secondary hydration reaction. This would result in the production of more hydration products, which would fill the pores and improve the pore structure. Therefore, an appropriate increase in the alkali equivalent of the alkali activator is also favorable to the optimization of the pore structure.

4.1.3. Effect of curing conditions on pore structure

The capillary pores are filled gradually as the hydration reaction progresses, which results in the decrease of the total porosity and the increase of the density of the concrete. Nonetheless, the curing condition is essential to ensure the hydration of the concrete and therefore, highly important for analyzing the pore structure.

An increase of the curing temperature is favorable to the dissolution of the slag and the hydration reaction and to the increase of crystallinity of the hydration products. This causes their distribution to become more uniform and in turn, improves the pore structure. Ju et al. [115] performed a comparative study of the effect of the curing temperatures −10 and 20 °C on the pore structure of AASC. They reported that as the temperature increased, the proportion of gel pores increased and that of macropores decreased, and the pore structure improved significantly. Wei et al. [123] studied the effect of low temperature on the pore structure of alkali activated slag/fly ash concrete, and they found that when the curing temperature was −5 °C, there were more harmful pores and larger porosity in the alkali-activated slag/fly ash concrete, while there were more harmless pores and smaller porosity when the curing temperature was 20 °C, as shown in Fig. 20. Gu et al. [124] performed a comparative study of the effect of the curing temperatures 7 and 20 °C on the pore structure of AASC. They observed that for an identical age, AASC cured at 20 °C had lower total porosity and a finer pore size distribution, albeit with a larger mesopore volume (Fig. 21). Aydın and Baradan [83] studied the effect of curing methods on the pore structure of AASC and investigated the idea that the pore size distribution of AASC subjected to autoclave curing was better than that of AASC subjected to steam curing.

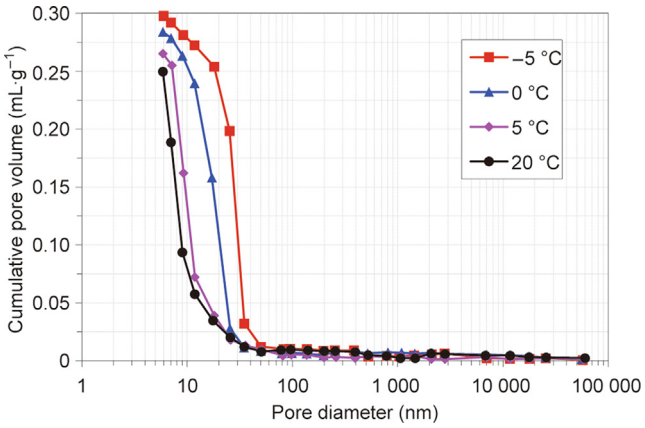

Fig. 20. Pore size distribution of alkali-activated slah/fly ash concrete at different temperatures (28 days) [123].

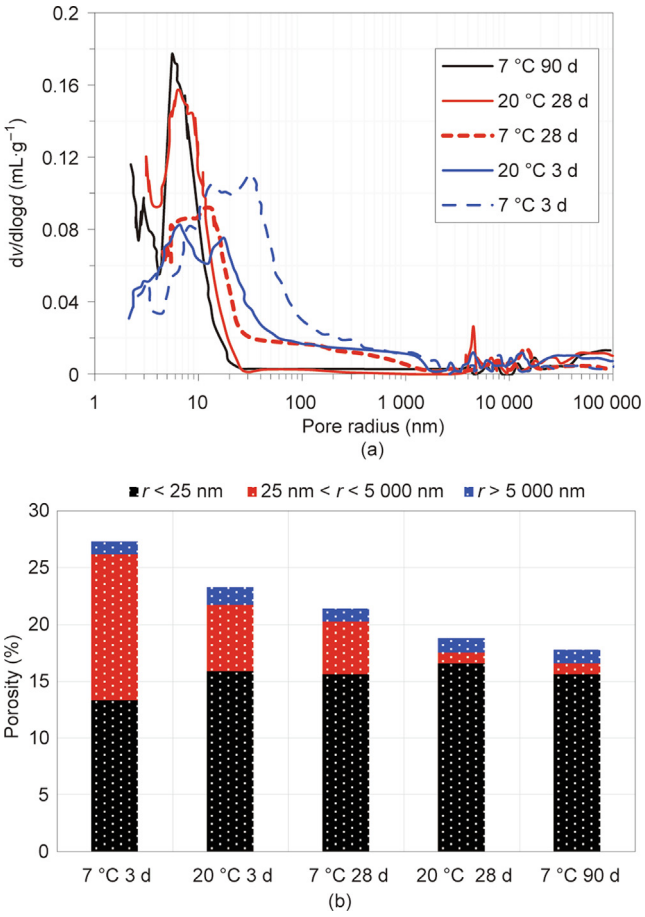

Fig. 21. (a) Pore size distribution and (b) classified porosity of AASC with different curing temperatures [124]. *r* is pore radius.

The effect of curing conditions on the pore structure of AASC can be summarized as follows. With an increase of the curing temperature, more hydration products are produced, the pores are filled better, the pore structure is optimized, and the microstructure is improved. However, with an excessive temperature, the pore water would be lost, and the drying shrinkage would be increased. Thereby, an unfavorable porous structure is formed, and the permeability is increased, which consequently degrades the pore structure of the AASC.

4.2. Interfacial transition zone (ITZ)

The sizes of slag particles and aggregate are different orders of magnitude, that is, the size of the aggregate is significantly larger than that of slag. Therefore, each type of aggregate exists as a mini "wall" in concrete. The packing of grains through the surface of aggregate is disrupted during the mixing process, which is the so-called "wall effect." Therefore, a zone with a deficit of huge grains that cannot physically pack adjacent to the aggregate is generated. This is the origin of the ITZ (Fig. 22) [125]. An ITZ rich in reaction products is generated in AASC due to the higher effective local water–binder ratio in this zone. The m_{Ca}/m_{Si+Na} mass ratio in the ITZ is low, and the generation of the hydration product N–A–S–H occurs rather than expansion Al-free cementation, which is conducive to the bonding of the ITZ and the matrix [126,127].

4.2.1. Effect of slag composition on ITZ

The ITZ between aggregate and cement paste is the weakest zone in concrete, which controls the important properties of concrete such as strength, permeability, and durability [128–131]. Therefore, the dense ITZ plays a significantly important role in improving the performance of AASC, which depends enormously on the composition of the slag.

Many factors affect the ITZ of AASC, such as the reaction between silica aggregate and alkaline aluminosilicate, the formation of additional reaction products on the surface of the aggregate, and the control of the condensation reaction by the alkali activator. The first two factors are both related to the slag composition. Yang et al. [96] studied the effect of adding nano-TiO_2 to the slag on the ITZ of AASC. It was found that the addition caused the porous C–S–H outside the AASC to become denser, the internal hydration products to be arranged compactly, the width and the quantity of the microcracks to be decreased, and the ITZ to become denser. Ju et al. [115] studied the influence of CaO in slag on the ITZ of AASC. They observed that after the CaO was incorporated, the edges of the GGBFS became smoother, and most of the GGBFS was surrounded by hydration products. Similarly, the addition of nano-SiO_2 also caused the ITZ of the AASC to become smoother [116]. Gruskovnjak et al. [53] studied the influence of different Al_2O_3 contents in slag on the ITZ of AASC. The slag with a high content of Al_2O_3 caused the AASC to form a hexagonal prismatic AFt that grew perpendicular to the surface of the slag. Furthermore, the AFt could be closely combined with the network C–S–H in the matrix. However, the slag with a low Al_2O_3 content was surrounded only by a thin hydration product layer, which still had a large pore space and poor ITZ. In addition to the slag composition, the fineness of slag is an important factor that affects the pore structure of AASC. Previous studies [132,133] demonstrated that the slag distribution became more uniform with the increase of the slag fineness. In addition, the fine particles had a better filling effect and more nucleation sites, whereby the hydration reaction was accelerated, and more hydration products were produced. This, in turn, caused the pores to be better filled and the internal ITZ to be smoother.

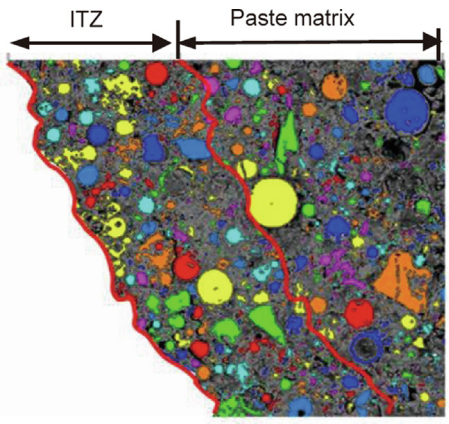

Fig. 22. Particle distribution in ITZ. Reproduced from Ref. [125] with permission.

The effect of the slag composition on the ITZ can be summarized as follows. The slag composition can affect the characteristics of the hydration products, which constitute an important standard for evaluating the quality of the ITZ. Therefore, slag composition is of high significance to the analysis of the ITZ of AASC. CaO, SiO_2, and Al_2O_3 are essential reactants for the formation of hydration products, and their content affects the formation of the hydration products. The addition of nano-CaO is favorable to the formation of C–(A)–S–H, and the reaction of CaO and H_2O is exothermic. These can accelerate the hydration reaction, produce more hydration products, and improve the ITZ [115]. Although nano-SiO_2 can reduce the alkalinity of pore solution, the unsaturated silicon bonds in nano-SiO_2 can react with OH– to form ≡Si–OH. Then, ≡Si–OH can react with $Ca(OH)_2$ to form C–S–H, which can effectively fill the pores and improve the ITZ [116,134,135]. Slag with a high Al_2O_3 content is favorable to the formation of AFt that is closely combined with the networked C–S–H. AFt is needle-shaped and has a large specific surface area, which can effectively fill the pores and thereby cause the ITZ to be denser. The fineness of slag is also a highly important factor that affects the ITZ. Nanomaterials have a substantial effect on the filling of pores and the nucleation effect of hydration products, and they can effectively reduce the shrinkage of AASC. Therefore, improving the fineness of slag is also highly important for enhancing the ITZ of AASC.

4.2.2. Effect of alkali activator on the ITZ

As mentioned previously, an alkali activator can produce hydration products with good morphology by influencing the condensation reaction or providing ions required for specific hydration products. Therefore, the alkali activator affects the ITZ of AASC. Zhang et al. [117] compared the effects of NaOH and Na_2SiO_3 on the ITZ of AASC, as shown in Fig. 23. The mass ratio of m_{Ca}/m_{Si} in C–(A)–S–H was lower, the degree of polymerization was higher, the hydration products were denser, and the ITZ of the AASC was more uniform and narrower when Na_2SiO_3 was used as the alkali activator compared with NaOH. Rashad et al. [69] studied the effect of Na_2SO_4 concentration on the ITZ of AASC. It was found that compared with the low concentration of Na_2SO_4 as the alkali activator, more needle-like AFt appeared in AASC when a higher concentration of Na_2SO_4 was used as the alkali activator, and the ITZ had better compactness.

The effect of the alkali activator on the ITZ of AASC can be summarized as follows. Na_2SiO_3 can provide more SiO_4^{4-}, which results in the decrease of m_{Ca}/m_{Si} mass ratio of the C–A–S–H and in turn, causes the formation of C–A–S–H with a higher degree of polymerization. This increases the disorder of the network structure and causes the C–A–S–H to be denser, which can better fill the pores and optimize the ITZ. Although the pH value of an NaOH solution

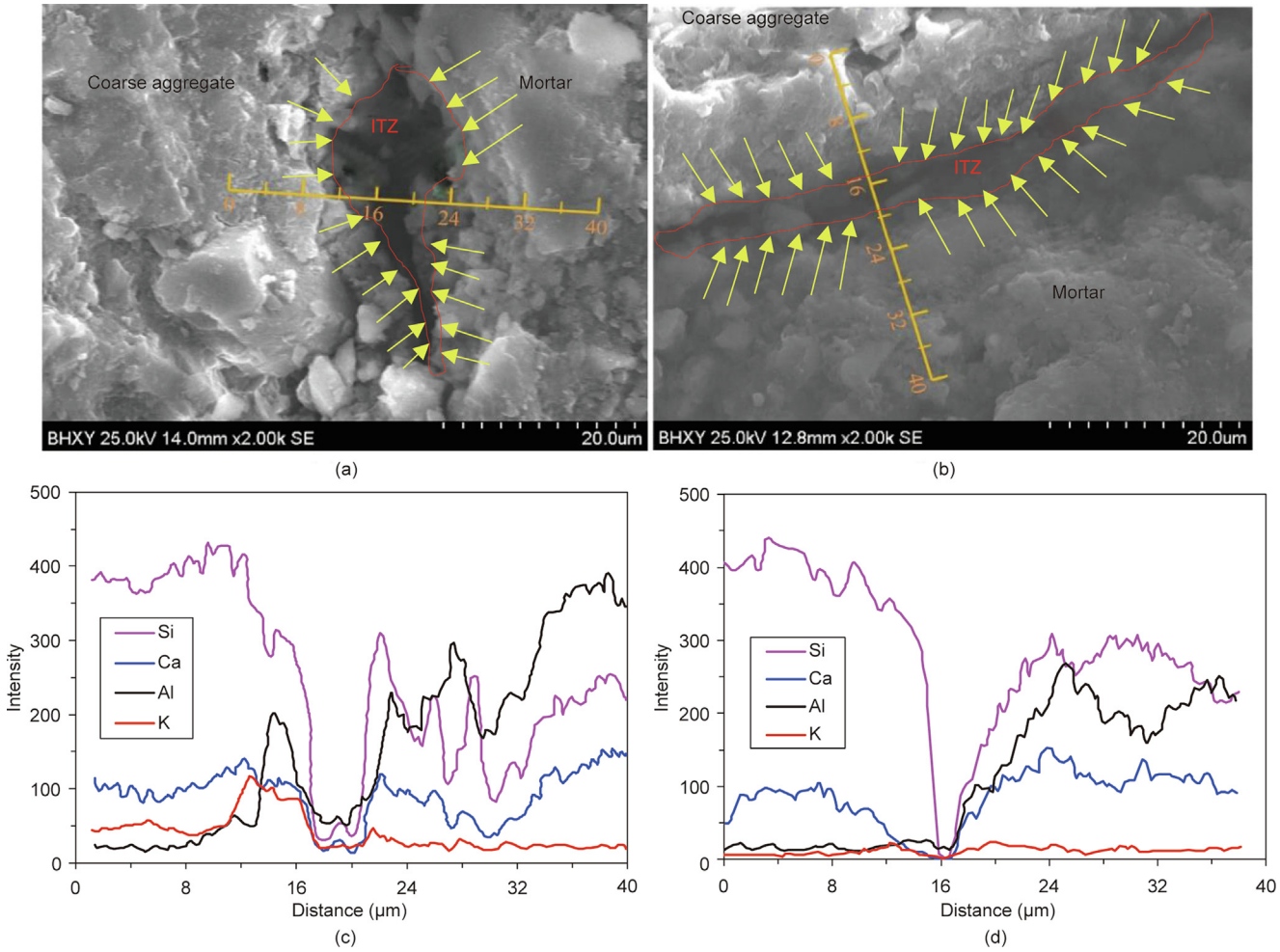

Fig. 23. Scanning electron microscope (SEM) images of the ITZ between coarse aggregate and mortar of (a) SH and (b) WG, and energy-dispersive X-ray spectroscopy (EDS) spectrum of the ITZ of (c) SH and (d) WG. Reproduced from Ref. [117] with permission.

is the highest and the hydration reaction is the fastest with an identical alkali equivalent, the excessively fast hydration reaction would cause a non-uniform distribution of hydration products, which would result in a rough ITZ. Fine needle-shaped AFt crystals appear in the hydration products of AASC as the hydration age increases when Na_2SO_4 is used as the alkali activator. AFt fills in the pores of AASC to make the structure denser, which decreases the porosity and improves the microstructure. Therefore, the ITZ of AASC in the subsequent curing period is better when Na_2SO_4 is used as the alkali activator compared with NaOH.

4.2.3. Effect of curing conditions on the ITZ

The increase of the curing temperature can accelerate the dissolution of slag, the progress of the hydration reaction, and the formation of hydration products. Therefore, the transition of the ITZ is smoother. Gu et al. [124] studied the effect of the curing temperature on the ITZ of AASC. The study determined that the ITZ of AASC became denser, and the unreacted slag could be detected when the curing temperature increased from 7 to 20 °C. Gebregziabiher et al. [75] also studied the effect of temperature on the ITZ of AASC. The study determined that the transition between the internal products and the unreacted slag of AASC was gentler and more abundant nucleation sites and fewer pores were apparent when the curing temperature was 50 °C compared with 23 °C. Many microcracks were observed in the above studies, which may have been caused by the drying shrinkage of the sample. Furthermore, the microcrack could be improved by adding expansion agents or shrinkage reducing agents [49,136]. In conclusion, the microstructure changes from loose particles to a dense structure with the increase in the curing temperature can be attributed to the improvement of the slag hydration reaction.

In recent years, there have been more and more research on the hydration characteristics and microstructure of AASC, and the understanding has become more profound, but there are still many problems to be solved. For example: ① Slag is a byproduct of the metallurgical industry whose composition fluctuates greatly, so the choice of slag is also a difficult problem. ② In general, a liquid activator is the first choice for an AASC activator. However, the dissolution of a solid activator can release heat and accelerate the dissolution and hydration reaction of slag, so a solid activator may also be used in actual engineering. Yet, there is a lack of a deeper understanding of solid activators. ③ Owing to the low fineness of slag, there are many gel pores and small pores in AASC, and this easily leads to the formation of the drying shrinkage of AASC. At present, expansion agents, air-entraining agents, and super absorbent resins [137], and so forth can be used to reduce the drying shrinkage, but this will affect the strength of AASC. The method that can reduce the drying shrinkage of AASC without affecting the strength and other properties of AASC is the focus of future research. ④ Compared with OPCC, AASC is more likely to have an

alkali-aggregate reaction due to the influence of an alkali activator, which can expand the pores and crack or even damage the matrix, especially when the aggregate also has alkali activity. Therefore, effective measures should be taken to limit alkali-aggregate reactions.

5. Conclusions

In this paper, the research results for the hydration characteristics and microstructure of AASC obtained in recent years are reviewed systematically. The effects of the slag composition, the type and dosage of the alkali activator, and curing conditions on the hydration characteristics and microstructure of AASC are summarized, as follows:

(1) The hydration process of AASC is affected by the composition of the slag, the type and dosage of the alkali activator, and the curing conditions. A variation in the composition of the slag can affect the activity of the slag hydration reaction and alter the rate of the hydration reaction. The alkali activator affects the dissolution and condensation reaction of the slag (mainly through the pH value) and thereby affects the hydration process of the AASC. The curing conditions can affect the rate of the hydration reaction and the breaking of old bonds during the polymerization reaction and ultimately, affect the hydration process of the AASC.

(2) The main hydration product of AASC is C–(A)–S–H with a relatively low m_{Ca}/m_{Si} mass ratio, mixed with C–(N)–A–S–H and N–A–S–H. However, the secondary hydration products change with the variations of the slag composition, alkali activator, and curing conditions. As the precursor of the hydration reaction, the slag composition directly affects the types of hydration products. Alkali activators can affect the dissolution of slag and provide the ions required for specific reaction products. Curing conditions can alter the crystallinity of hydration products and then generate different forms of hydration products.

(3) Different slag compositions can produce hydration products with different porosities, and the fineness of slag can affect the nucleation of the hydration products and alter the uniformity of the hydration products. An alkali activator can provide specific ions for the hydration reaction with dissolved slag, which can increase the quantity of hydration products or produce precipitation products that can better fill the pores and reduce the porosity. Curing conditions can affect the production of hydration products and vary the uniformity of the hydration products. However, an excessive temperature would destroy the structure of the hydration products and cause the surface of these products to be rougher. Therefore, an excessive temperature is not conducive to the development of the pore structure.

(4) The ITZ is the weakest zone in concrete. The slag composition, alkali activator, and curing conditions can alter the morphology of the hydration products, the smoothness of the transition between internal hydration products and external hydration products, and the nucleation sites of hydration products. Although the hydration heat of AASC is lower than that of OPCC, AASC can form a denser ITZ, which can be attributed to the high degree of polymerization and the generation of more ordered C–A–S–H and N–A–S–H. With regard to the use of an identical alkali equivalent of NaOH, Na_2SiO_3, or Na_2SO_4 as the alkali activator for AASC, the quantity of hydration products generated is the largest and the ITZ is the densest for Na_2SiO_3. This is followed by NaOH and Na_2SO_4, in that order.

Overall, AASC has better durability and mechanical properties than OPCC and it has broad application prospects. However, the research on hydration kinetics, the formation of hydration products, the improvement of the pore structure, the ITZ, and other mechanisms is not adequate. Furthermore, AASC also has the disadvantages of low dry shrinkage performance and low liquidity. Therefore, more research is required to better understand AASC and to solve the problems related to it for AASC to be a preferable substitute for ordinary cement-based materials.

Acknowledgments

The authors would like to acknowledge the National Natural Science Foundation of China (51590914 and 51608432), and Natural Science Foundation of Shaanxi Province (2019JQ-481).

Compliance with ethical guidelines

Qiang Fu, Mengxin Bu, Zhaorui Zhang, Wenrui Xu, Qiang Yuan, and Ditao Niu declare that they have no conflicts of interest or financial conflicts to disclose.

References

[1] Hardjito D, Wallah S, Sumajouw D, Rangan B. On the development of fly ash-based geopolymer concrete. ACI Mater J 2004;101:467–72.
[2] Mehta PK. Greening of the concrete industry for sustainable development. Concr Int 2002;24(7):23–9.
[3] Vázquez-Rowe I, Ziegler-Rodriguez K, Laso J, Quispe I, Aldaco R, Kahhat R. Production of cement in Peru: understanding carbon-related environmental impacts and their policy implications. Resour Conserv Recycling 2019;142:283–92.
[4] Uwasu M, Hara K, Yabar H. World cement production and environmental implications. Environ Dev 2014;10:36–47.
[5] Abdalqader AF, Jin F, Al-Tabbaa A. Development of greener alkali-activated cement: utilisation of sodium carbonate for activating slag and fly ash mixtures. J Clean Prod 2016;113:66–75.
[6] Cabeza LF, Barreneche C, Miró L, Morera J, Bartolí E, Inés FA. Low carbon and low embodied energy materials in buildings: a review. Renew Sustain Energy Rev 2013;23:536–42.
[7] Fernández-Jiménez A, Palomo JG, Puertas F. Alkali-activated slag mortars: mechanical strength behaviour. Cement Concr Res 1999;29(8):1313–21.
[8] Chithiraputhiran S, Neithalath N. Isothermal reaction kinetics and temperature dependence of alkali activation of slag, fly ash and their blends. Constr Build Mater 2013;45(7):233–42.
[9] Chang JJ. A study on the setting characteristics of sodium silicate-activated slag pastes. Cement Concr Res 2003;33(7):1005–11.
[10] Altan E, Erdoğan ST. Alkali activation of a slag at ambient and elevated temperatures. Cement Concr Compos 2012;34(2):131–9.
[11] Shi C, Roy D, Krivenko P. Alkali-activated cements and concretes. Los Angeles: CRC Press; 2006.
[12] Zhang YJ, Yang MY, Kang L, Zhang L, Zhang K. Research progresses of new type alkali-activated cementitious material catalyst. J Inorg Mater 2016;31(3):225–33.
[13] Bakharev T, Sanjayan JG, Cheng YB. Alkali activation of Australian slag cements. Cement Concr Res 1999;29(1):113–20.
[14] Bakharev T, Sanjayan JG, Cheng YB. Sulfate attack on alkali-activated slag concrete. Cement Concr Res 2002;32(2):211–6.
[15] Bakharev T, Sanjayan JG, Cheng YB. Resistance of alkali-activated slag concrete to acid attack. Cement Concr Res 2003;33(10):1607–11.
[16] Miller SA, John VM, Pacca SA, Horvath A. Carbon dioxide reduction potential in the global cement industry by 2050. Cement Concr Res 2018;114:115–24.
[17] Garcia-Lodeiro I, Fernández-Jimenez A, Pena P, Palomo A. Alkaline activation of synthetic aluminosilicate glass. Ceram Int 2014;40(4):5547–58.
[18] Provis JL, van Deventer JSJ. Alkali activated materials, RILEM state-of-the-art reports 13. Dordrecht: Springer; 2014.
[19] Schilling PJ, Roy A, Eaton HC, Malone PG, Brabston WN. Microstructure, strength, and reaction products of ground granulated blast-furnace slag activated by highly concentrated NaOH solution. J Mater Res 1994;9(1):188–97.
[20] Fang S, Lam ESS, Li B, Wu B. Effect of alkali contents, moduli and curing time on engineering properties of alkali activated slag. Constr Build Mater 2020;249:118799.
[21] Roy DM, Silsbee MR, Wolfe-Confer D. New rapid setting alkali activated cement compositions. MRS Online Proc Libr 1989;179:179–203.
[22] Stone MD, Hunsucker DQ. Construction and interim performance of a pyrament cement concrete bridge deck. Report. Lexington: Kentucky Transportation Center; 1993 Jun. Report No.: KTC-93-17.
[23] Zhang P, Wang K, Li Q, Wang J, Ling Y. Fabrication and engineering properties of concretes based on geopolymers/alkali-activated binders–a review. J Clean Prod 2020;258:120896.
[24] Tänzer R, Buchwald A, Stephan D. Effect of slag chemistry on the hydration of alkali-activated slag: comparison with ordinary Portland cement blast-furnace slag. Mater Struct 2015;48(3):629–41.

[25] Bellmann F, Stark J. Activation of blast furnace slag by a new method. Cement Concr Res 2009;39(8):644–50.
[26] Manjunath R, Narasimhan MC, Umesh K, Kumar S, Bala Bharathi UK. Studies on development of high performance, self-compacting alkali activated slag concrete mixes using industrial wastes. Constr Build Mater 2019;198:133–47.
[27] Glukhovsky VD, Rostovkaya GS, Rumyna GV. High strength slag-alkali cement. In: Proceedings of the 7th International Congress on the Chemistry of Cements; 1980 Jan 1; Paris, France. Paris: Editions Septima; 1980.
[28] Turner LK, Collins FG. Carbon dioxide equivalent (CO_2-e) emissions: a comparison between geopolymer and OPC cement concrete. Constr Build Mater 2013;43:125–30.
[29] Soriano L, Font A, Tashima MM, et al. Almond-shell biomass ash (ABA): a greener alternative to the use of commercial alkaline reagents in alkali-activated cement. Constr Build Mater. 2021;290:123351.
[30] Bernal SA, Mejía de Gutiérrez R, Pedraza AL, PROVIS J, Rodriguez ED, Delvasto S. Effect of binder content on the performance of alkali-activated slag concretes. Cement Concr Res 2011;41(1):1–8.
[31] Jamieson E, Kealley CS, van Riessen A, Hart RD. Optimising ambient setting bayer derived fly ash geopolymers. Materials 2016;9(5):392.
[32] Xu F, Wei H, Qian W, Cai Y. Composite alkaline activator on cemented soil: multiple tests and mechanism analyses. Constr Build Mater 2018;188:433–43.
[33] Alonso S, Palomo A. Alkaline activation of metakaolin and calcium hydroxide mixtures: influence of temperature, activator concentration and solids ratio. Mater Lett 2001;47(1–2):55–62.
[34] Mehdizadeh H, Najafi Kani E, Sanchez AP, Fernandez-Jimenez A. Rheology of activated phosphorus slag with lime and alkaline salts. Cement Concr Res 2018;113:121–9.
[35] Kaur K, Singh J, Kaur M. Compressive strength of rice husk ash based geopolymer: the effect of alkaline activator. Constr Build Mater 2018;169:188–92.
[36] Jin Y, Feng W, Zheng D, Dong Z, Cui H, Li M, et al. Study on the interaction mechanism between slags and alkali silicate activators: a hydration kinetics approach. Constr Build Mater 2020;250:118900.
[37] Yu L. Study on the preparation and performance of alkali-activated slag cementitious materials [dissertation]. Zhengzhou: Zhengzhou University; 2010. Chinese.
[38] Zheng JR, Yao ZY, Liu LN. Experimental study on chemical shrinkage or expansion of alkali activated cementitious materials. Bull Chin Ceram Soc 2009;28(1):49–53. Chinese.
[39] Collins F, Sanjayan JG. Microcracking and strength development of alkali activated slag concrete. Cement Concr Compos 2001;23(4–5):345–52.
[40] Angulo-Ramírez DE, Mejía de Gutiérrez R, Puertas F. Alkali-activated Portland blast-furnace slag cement: mechanical properties and hydration. Constr Build Mater 2017;140:119–28.
[41] Fernández-Jiménez A, Puertas F. Alkali-activated slag cements: kinetic studies. Cement Concr Res 1997;27(3):359–68.
[42] Fernandez-Jimenez A, Puertas F, Arteaga A. Determination of kinetic equations of alkaline activation of blast furnace slag by means of calorimetric data. J Therm Anal Calorim 1998;52(3):945–55.
[43] Bernal SA, Provis JL, Rose V, Mejía de Gutierrez R. Evolution of binder structure in sodium silicate-activated slag-metakaolin blends. Cement Concr Compos 2011;33(1):46–54.
[44] Deir E, Gebreziabiher BS, Peethamparan S. Influence of starting material on the early age hydration kinetics and composition of binding gel in alkali activated binder systems. Cement Concr Compos 2014;48:108–17.
[45] Altan E, Erdogan ST. Alkali activation of a slag at ambient and elevated temperatures. Cement Concr Compos 2012;34(2):131–9.
[46] Haha MB, Lothenbach B, Le Saout G, Winnefeld F. Influence of activator type on hydration kinetics, hydrate assemblage and microstructural development of alkali activated blast furnace slags. Cement Concr Res 2012;42(1):74–83.
[47] Krizan D, Zivanovic B. Effects of dosage and modulus of water glass on early hydration of alkali-slag cements. Cement Concr Res 2002;32(8):1181–8.
[48] Shi C, Day RL. Some factors affecting early hydration of alkali-slag cements. Cement Concr Res 1996;26(3):439–47.
[49] Brough AR, Atkinson A. Sodium silicate-based, alkali-activated slag mortars: part I. strength, hydration and microstructure. Cement Concr Res 2002;32(6):865–79.
[50] Bakharev T, Sanjayan JG, Cheng YB. Effect of elevated temperature curing on properties of alkali-activated slag concrete. Cement Concr Res 1999;29(10):1619–25.
[51] Haha MB, Lothenbach B, Le Saout G, Winnefeld F. Influence of slag chemistry on the hydration of alkali-activated blast-furnace slag—part II: effect of Al_2O_3. Cement Concr Res 2012;42(1):74–83.
[52] Wang SD, Scrivener KL, Pratt PL. Factors affecting the strength of alkali-activated slag. Cement Concr Res 1994;24(6):1033–43.
[53] Gruskovnjak A, Lothenbach B, Winnefeld F, Figi R, Ko SC, Adler M, et al. Hydration mechanisms of supersulfated slag cements. Cement Concr Res 2008;38(7):983–92.
[54] Sakulich AR, Anderson E, Schauer CL, Barsoum MW. Influence of Si:Al ratio on the microstructural and mechanical properties of a fine-limestone aggregate alkali-activated slag concrete. Mater Struct 2010;43(7):1025–35.
[55] Haha MB, Lothenbach B, Le Saout G, et al. Influence of slag chemistry on the hydration of alkali-activated blast-furnace slag—Part I: effect of MgO. Cement Concr Res 2011;41(9):955–63.
[56] Bernal SA, San Nicolas R, Myers RJ, Mejía de Gutiérrez R, Puertas F, van Deventer JSJ, et al. MgO content of slag controls phase evolution and structural changes induced by accelerated carbonation in alkali-activated binders. Cement Concr Res 2014;57:33–43.
[57] Ke X, Bernal SA, Provis JL. Controlling the reaction kinetics of sodium carbonate-activated slag cements using calcined layered double hydroxides. Cement Concr Res 2016;81:24–37.
[58] Katyal NK, Ahluwalia SC, Parkash R. Effect of TiO_2 on the hydration of tricalcium silicate. Cement Concr Res 1999;29(11):1851–5.
[59] Wassing W. Relationship between the chemical reactivity of granulated blast furnace slags and the mortar standard compressive strength of the blast furnace cements produced from them. Chem Int 2003;1(5):95–109.
[60] Li C, Sun H, Li L. A review: the comparison between alkali-activated slag (Si + Ca) and metakaolin (Si + Al) cements. Cement Concr Res 2010;40(9):1341–9.
[61] Cao RL, Zhang SQ, Banthia N, Zhang Y, Zhang Z. Interpreting the early-age reaction process of alkali-activated slag by using combined embedded ultrasonic measurement, thermal analysis, XRD, FTIR and SEM. Compos Part B Eng 2020;186:107840.
[62] Shi C, Day RL. A calorimetric study of early hydration of alkali-slag cements. Cement Concr Res 1995;25(6):1333–46.
[63] Pacheco-Torgal F, Castro-Gomes J, Jalali S. Alkali-activated binders: a review. Part 1. historical background, terminology, reaction mechanisms and hydration products. Constr Build Mater 2008;22(7):1305–14.
[64] Gijbels K, Pontikes Y, Samyn P, Schreurs S, Schroeyers W. Effect of NaOH content on hydration, mineralogy, porosity and strength in alkali/sulfate-activated binders from ground granulated blast furnace slag and phosphogypsum. Cement Concr Res 2020;132:106054.
[65] Li N, Shi C, Zhang Z. Understanding the roles of activators towards setting and hardening control of alkali-activated slag cement. Compos Part B Eng 2019;171:34–45.
[66] Roy DM. Alkali-activated cements opportunities and challenges. Cement Concr Res 1999;29(2):249–54.
[67] Tan HB, Deng XF, He XY, Zhang J, Zhang X, Su Y, et al. Compressive strength and hydration process of wet-grinded granulated blast-furnace slag activated by sodium sulfate and sodium carbonate. Cement Concr Compos 2019;97:387–98.
[68] Mobasher N, Bernal SA, Provis JL. Structural evolution of an alkali sulfate activated slag cement. J Nucl Mater 2016;468:97–104.
[69] Rashad AM, Bai Y, Basheer PAM, Milestone NB, Collier NC. Hydration and properties of sodium sulfate activated slag. Cement Concr Compos 2013;37:20–9.
[70] Provis JL, Bernal SA. Geopolymers and related alkali-activated materials. Annu Rev Mater Res 2014;44(1):299–327.
[71] Bernal SA, Provis JL, Myers RJ, San Nicolas R, van Deventer JSJ. Role of carbonates in the chemical evolution of sodium carbonate-activated slag binders. Mater Struct 2015;48(3):517–29.
[72] Kim JC, Hong SY. Liquid concentration changes during slag cement hydration by alkali activation. Cement Concr Res 2001;31(2):283–5.
[73] Ravikumar D, Neithalath N. Reaction kinetics in sodium silicate powder and liquid activated slag binders evaluated using isothermal calorimetry. Thermochim Acta 2012;546:32–43.
[74] Zhou H, Wu X, Xu Z, Tang M. Kinetic study on hydration of alkali-activated slag. Cement Concr Res 1993;23(6):1253–8.
[75] Gebregziabiher BS, Thomas RJ, Peethamparan S. Temperature and activator effect on early-age reaction kinetics of alkali-activated slag binders. Constr Build Mater 2016;113:783–93.
[76] Gebregziabiher BS, Thomas R, Peethamparan S. Very early-age reaction kinetics and microstructural development in alkali-activated slag. Cement Concr Compos 2015;55:91–102.
[77] Rothstein D, Thomas JJ, Christensen BJ, Jennings HM. Solubility behavior of Ca-, S-, Al-, and Si-bearing solid phases in Portland cement pore solutions as a function of hydration time. Cement Concr Res 2002;32(10):1663–71.
[78] Fernández-Jiménez A, Puertas F. Effect of activator mix on the hydration and strength behaviour of alkali-activated slag cements. Adv Cement Res 2003;15(3):129–36.
[79] Song S, Sohn D, Jennings HM, Mason TO. Hydration of alkali-activated ground granulated blast furnace slag. J Mater Sci 2000;35(1):249–57.
[80] Gruskovnjak A, Lothenbach B, Holzer L, Figi R, Winnefeld F. Hydration of alkali-activated slag: comparison with ordinary Portland cement. Adv Cement Res 2006;18(3):119–28.
[81] Sohn SD, Jennings HM. Pore solution chemistry of alkali-activated ground granulated blast-furnace slag. Cement Concr Res 1999;29(2):159–70.
[82] Živica V. Effects of type and dosage of alkaline activator and temperature on the properties of alkali-activated slag mixtures. Constr Build Mater 2007;21(7):1463–9.
[83] Aydın S, Baradan B. Mechanical and microstructural properties of heat cured alkali-activated slag mortars. Mater Des 2012;35:374–83.
[84] Fernández-Jiménez A, Puertas F. Influence of the activator concentration on the kinetics of the alkaline activation process of a blast-furnace slag. Mater Constr 2010;47:246.
[85] Wang SD, Pu XC, Scrivener KL, Pratt PL. Alkali-activated slag cement and concrete: a review of properties and problems. Adv Cement Res 1995;7(27):93–102.
[86] Fernández-Jiménez A, Puertas F, Sobrados I, Sanz J. Structure of calcium silicate hydrates formed in alkaline-activated slag: influence of the type of alkaline activator. J Am Ceram Soc 2003;86(8):1389–94.

[87] Myers RJ, Bernal SA, San Nicolas R, Provis JL. Generalized structural description of calcium-sodium aluminosilicate hydrate gels: the cross-linked substituted tobermorite model. Langmuir 2013;29(17):5294–306.
[88] Richardson IG, Brough AR, Groves GW, Dobson CM. The characterization of hardened alkali-activated blast-furnace slag pastes and the nature of the calcium silicate hydrate (C–S–H) paste. Cement Concr Res 1994;24(5):813–29.
[89] Puertas F, Palacios M, Manzano H, Dolado JS, Rico A, Rodríguez J. A model for the C–A–S–H gel formed in alkali-activated slag cements. J Eur Ceram Soc 2011;31(12):2043–56.
[90] Jiang DB, Li XG, Lv Y, Li CJ, Jiang WG, Liu ZL, et al. Autogenous shrinkage and hydration property of alkali activated slag pastes containing superabsorbent polymer. Cement Concr Res. 2021;149:106581.
[91] Wang SD, Scrivener KL. Hydration products of alkali-activated slag cement. Cement Concr Res 1995;25(3):561–71.
[92] Bernal SA, Provis JL, Walkley B, San Nicolas R, Gehman JD, Brice DG, et al. Gel nanostructure in alkali-activated binders based on slag and fly ash, and effects of accelerated carbonation. Cement Concr Res 2013;53:127–44.
[93] Bernal SA, de Gutierrez RM, Provis JL, Rose V. Effect of silicate modulus and metakaolin incorporation on the carbonation of alkali silicate-activated slags. Cement Concr Res 2010;40(6):898–907.
[94] Zhang YJ, Zhao YL, Li HH, Xu DL. Structure characterization of hydration products generated by alkaline activation of granulated blast furnace slag. J Mater Sci 2008;43(22):7141–7.
[95] Puertas F, Palacios M, Manzano H, et al. C–A–S–H gels formed in alkali-activated slag cement pastes. Structure and effect on cement properties and durability. Matec Web Conf 2014;11:01002.
[96] Yang LY, Jia ZJ, Zhang YM, Dai JG. Effects of nano-TiO_2 on strength, shrinkage and microstructure of alkali activated slag pastes. Cement Concr Compos 2015;57:1–7.
[97] Schilling PJ, Butler LG, Roy A, Eaton HC. ^{29}Si and ^{27}Al MAS-NMR of NaOH-activated blast-furnace slag. J Am Ceram Soc 1994;77(9):2363–8.
[98] Richardson IG. Tobermorite/jennite- and tobermorite/calcium hydroxide-based models for the structure of C–S–H: applicability to hardened pastes of tricalcium silicate, β-dicalcium silicate, Portland cement, and blends of Portland cement with blast-furnace slag, metakaolin, or silica fume. Cement Concr Res 2004;34(9):1733–77.
[99] Pardal X, Brunet F, Charpentier T, Pochard I, Nonat A. ^{27}Al and ^{29}Si solid-state NMR characterization of calcium-aluminosilicate-hydrate. Inorg Chem 2012;51(3):1827–36.
[100] Renaudin G, Russias J, Leroux F, Cau-dit-Coumes C, Frizon F. Structural characterization of C–S–H and C–A–S–H samples-part II: local environment investigated by spectroscopic analyses. J Solid State Chem 2009;182(12):3320–9.
[101] Escalante-García J, Fuentes AF, Gorokhovsky A, Fraire-Luna PE, Mendoza-Suarez G. Hydration products and reactivity of blast-furnace slag activated by various alkalis. J Am Ceram Soc 2003;86(12):2148–53.
[102] Bonk F, Schneider J, Cincotto MA, Panepucci H. Characterization by multinuclear high-resolution NMR of hydration products in activated blast-furnace slag pastes. J Am Ceram Soc 2003;86(10):1712–9.
[103] Palacios M, Puertas F. Effect of carbonation on alkali-activated slag paste. J Am Ceram Soc 2006;89(10):3211–21.
[104] Häkkinen T. The influence of slag content on the microstructure, permeability and mechanical properties of concrete: part 1. microstructural studies and basic mechanical properties. Cement Concr Res 1993;23(2):407–21.
[105] Lothenbach B, Gruskovnjak A. Hydration of alkali-activated slag: thermodynamic modelling. Adv Cement Res 2007;19(2):81–92.
[106] Chen W, Brouwers H. The hydration of slag, part 1: reaction models for alkali-activated slag. J Mater Sci 2007;42(2):428–43.
[107] Mobasher N, Bernal SA, Kinoshita H, Provis JL. Gamma irradiation resistance of early age $Ba(OH)_2$–Na_2SO_4–slag cementitious grouts. J Nucl Mater 2016;482:266–77.
[108] Bai Y, Collier NC, Milestone NB, Yang CH. The potential for using slags activated with near neutral salts as immobilisation matrices for nuclear wastes containing reactive metals. J Nucl Mater 2011;413(3):183–92.
[109] Rashad AM, Bai Y, Basheer PAM, Collier NC, Milestone NB. Chemical and mechanical stability of sodium sulfate activated slag after exposure to elevated temperature. Cement Concr Res 2012;42(2):333–43.
[110] Shi C, Wu X, Tang M. Hydration of alkali-slag cements at 150 °C. Cement Concr Res 1991;21(1):91–100.
[111] Sugama T, Brothers L. Sodium-silicate-activated slag for acid-resistant geothermal well cements. J Adv Cem Res 2004;16(2):77–87.
[112] Jiang WM. Alkali-activated cementitious materials: mechanisms, microstructure and properties [dissertation]. University Park: The Pennsylvania State University; 1997.
[113] Palomo AJL, Shi C. Advances in understanding alkali-activated materials. Cement Concr Res 2015;78:110–25.
[114] Wang SY, Mccaslin E, White CE. Effects of magnesium content and carbonation on the multiscale pore structure of alkali-activated slags. Cement Concr Res 2020;130:105979.
[115] Ju C, Liu YS, Jia MJ, Yu K, Yu Z, Yang Y. Effect of calcium oxide on mechanical properties and microstructure of alkali-activated slag composites at sub-zero temperature. J Build Eng 2020;32:101561.
[116] Wang JB, Du P, Zhou ZH, Xu D, Xie N, Cheng X. Effect of nano-silica on hydration, microstructure of alkali-activated slag. Constr Build Mater 2019;220:110–8.
[117] Zhang Y, Wan X, Hou D, Zhao T, Cui Y. The effect of mechanical load on transport property and pore structure of alkali-activated slag concrete. Constr Build Mater 2018;189:397–408.
[118] Lee NK, Jang JG, Lee HK. Shrinkage characteristics of alkali-activated fly ash/slag paste and mortar at early ages. Cement Concr Compos 2014;53:239–48.
[119] Hu X, Shi CJ, Shi ZG, Zhang LY. Compressive strength, pore structure and chloride transport properties of alkali-activated slag/fly ash mortars. Cement Concr Compos 2019;104:103392.
[120] Hu X, Shi C, Liu X, Zhang Z. Studying the effect of alkali dosage on microstructure development of alkali-activated slag pastes by electrical impedance spectroscopy (EIS). Constr Build Mater 2020;261:119982.
[121] Ye HL, Fu CQ, Yang GJ. Influence of dolomite on the properties and microstructure of alkali-activated slag with and without pulverized fly ash. Cement Concr Compos 2019;103:224–32.
[122] Jiao ZZ, Wang Y, Zheng WZ, Huang W. Effect of the activator on the performance of alkali-activated slag mortars with pottery sand as fine aggregate. Constr Build Mater 2019;197:83–90.
[123] Wei XB, Li DQ, Ming F, Yang C, Chen L, Liu Y. Influence of low-temperature curing on the mechanical strength, hydration process, and microstructure of alkali-activated fly ash and ground granulated blast furnace slag mortar. Constr Build Mater 2021;269:121811.
[124] Gu YM, Fang YH, You D, Gong Y, Zhu C. Properties and microstructure of alkali-activated slag cement cured at below- and about-normal temperature. Constr Build Mater 2015;79:1–8.
[125] Fang GH, Zhang MZ. The evolution of interfacial transition zone in alkali-activated fly ash-slag concrete. Cement Concr Res 2020;129:105963.
[126] Brough AR, Atkinson A. Automated identification of the aggregate–paste interfacial transition zone in mortars of silica sand with Portland or alkali-activated slag cement paste. Cement Concr Res 2000;30(6):849–54.
[127] Nicolas RS, Bernal SA, Mejía de Gutiérrez R, van Deventer JSJ, Provis JL. Distinctive microstructural features of aged sodium silicate-activated slag concretes. Cement Concr Res 2014;65:41–51.
[128] Breton D, Carles-Gibergues A, Ballivy G, Grandet J. Contribution to the formation mechanism of the transition zone between rock–cement paste. Cement Concr Res 1993;23(2):335–46.
[129] Scrivener KL, Nemati KM. The percolation of pore space in the cement paste/aggregate interfacial zone of concrete. Cement Concr Res 1996;26(1):35–40.
[130] Cwirzen A, Penttala V. Aggregate-cement paste transition zone properties affecting the salt–frost damage of high-performance concretes. Cement Concr Res 2005;35(4):671–9.
[131] Leemann A, Münch B, Gasser P, Holzer L. Influence of compaction on the interfacial transition zone and the permeability of concrete. Cement Concr Res 2006;36(8):1425–33.
[132] Saedi M, Behfarnia K, Soltanian H. The effect of the blaine fineness on the mechanical properties of the alkali-activated slag cement. J Build Eng 2019;26:100897.
[133] Rakhimova NR, Rakhimov RZ, Naumkina NI, Khuzin AF, Osin YN. Influence of limestone content, fineness, and composition on the properties and microstructure of alkali-activated slag cement. Cement Concr Compos 2016;72:268–74.
[134] Xu Z, Zhou Z, Du P, Cheng X. Effects of nano-limestone on hydration properties of tricalcium silicate. J Therm Anal Calorim 2017;129(1):75–83.
[135] Qing Y, Zenan Z, Deyu K, Rongshen C. Influence of nano-SiO_2 addition on properties of hardened cement paste as compared with silica fume. Constr Build Mater 2007;21(3):539–45.
[136] Gu YM, Fang YH. Shrinkage, cracking, shrinkage reducing and toughening of alkali-activated slag cement–a short review. J Chin Ceram Soc 2012;40:76–84. Chinese.
[137] Li ZM, Wyrzykowski M, Dong H, Granja J, Azenha M, Lura P, et al. Internal curing by superabsorbent polymers in alkali-activated slag. Cement Concr Res 2020;135:106123.